Thermodynamic and turbomachinery design analysis of supercritical Brayton cycles for exhaust gas heat recovery

Uusitalo Antti, Ameli Alireza, Turunen-Saaresti Teemu

This is a Final draft version of a publication

published by Elsevier

in Energy

DOI: 10.1016/j.energy.2018.10.181

Please cite the publication as follows:

Uusitalo, A., Ameli, A., Turunen-Saaresti, T. (2018). Thermodynamic and turbomachinery design analysis of supercritical Brayton cycles for exhaust gas heat recovery. Energy, Vol. 167, ss. 60-79. DOI: 10.1016/j.energy.2018.10.181

Thermodynamic and turbomachinery design analysis of supercritical Brayton cycles for exhaust gas heat recovery

Antti Uusitalo, Alireza Ameli, Teemu Turunen-Saaresti

**Lappeenranta University of Technology, School of Energy Systems, P.O. Box 20, 53851 Lappeenranta, Finland*

Abstract

Significant amount of energy is wasted in engine systems as waste heat. In this study, the use of supercritical Brayton cycles for recovering exhaust gas heat of large-scale engines is investigated. The aim of the study is to investigate the electricity production potential with different operational conditions and working fluids, and to identify the main design parameters affecting the cycle power production. The studied process configurations are the simple recuperated cycle and intercooled recuperated cycle. As the performance of the studied cycle is sensitive on the turbomachinery design and efficiencies, the design of the process turbine and compressor were included in the analysis. Cycles operating with CO2 and ethane resulted in the highest performances in both the simple and intercooled cycle configurations, while the lowest cycle performances were simulated with ethylene and R116. 18.3 MW engine was selected as the case engine and maximum electric power output of 1.76 MW was simulated by using a low compressor inlet temperature, intercooling, and high turbine inlet pressure. It was concluded that working fluid and the cycle operational parameters have significant influence not only on the thermodynamic cycle design, but also highly affects the optimal rotational speed and geometry of the turbomachines.

Keywords: Supercritical Brayton Cycle, Waste heat recovery, Organic fluid, Energy efficiency, Turbomachinery design

Email address: `*Corresponding author: antti.uusitalo@lut.fi` (Antti Uusitalo, Alireza Ameli, Teemu Turunen-Saaresti)

Nomenclature

Latin alphabet

P	power	kW
c_p	specific heat capacity	kJ/kgK
h	specific enthalpy	kJ/kg
q_m	mass flow rate	kg/s
q_v	volumetric flow rate	m^3/s
p	pressure	bar
T	temperature	^{o}C
n	rotational speed	rpm
b	blade height	m
s	specific entropy	kJ/kgK
D	turbine diameter	m
Re	Reynolds number	-
x	Pressure rise factor	

Greek alphabet

η	efficiency	-
ϕ	heat rate	kW
Π	pressure ratio	-
ς	loss factor	-
κ	velocity ratio	-
μ	dynamic viscosity	Pas
ε	recuperator effectiveness	-

Abbreviations

CIT	Compressor inlet temperature
SBC	Supercritical Brayton Cycle
ORC	Organic Rankine cycle
CO_2	Carbon dioxide
WHR	Waste heat recovery
MDM	Octamethyltrisiloxane
R116	Hexafluoroethane

Subscripts

s	isentropic
c	cycle/compressor
comp1	compressor 1
comp2	compressor 2
wf	working fluid
in	inlet
out	outlet
e	electricity
eg	exhaust gas
h	heater
hub	blade hub
tip	blade tip
t	turbine
df	disk friction
pass	passage loss
0	turbine stator inlet
1	turbine stator outlet/rotor inlet
2	turbine rotor outlet
0’	compressor rotor inlet
1’	compressor rotor outlet

1. Introduction

During the last decades, several methods to increase efficiency and reduce emissions in different types of energy production processes have been studied and developed intensively. Converting waste heat into electricity has been identified as one of the most promising ways in achieving significant efficiency improvements and emission reductions in power production systems and industrial processes[1]. Despite the recent improvements in energy efficiency of large-scale engine power plants and marine engine systems, a large portion of the fuel power is still wasted in the process in a form of waste heat. When considering the waste heat recovery (WHR) in engine systems, the exhaust heat utilization contains the largest potential for improving energy efficiency of the whole system, due to the relatively high temperature level and large amount of waste heat, when compared to the other waste heat streams from the engine. Thus, most of the research efforts related to WHR in engine systems have been concentrating on the utilization of the exhaust gas heat[2].

The potential of recovering waste heat with different technologies has been intensively studied for engine systems at different power scales. The most widely used types of waste heat recovery systems are the conventional steam Rankine cycle or organic Rankine cycles (ORC) using an organic fluid as the working fluid. The use of ORC systems has been preferred instead of conventional steam Rankine cycles especially in low power output or low temperature waste heat recovery systems[3]. Kalina cycle using a mixture of water and ammonium as the working fluid has been also considered as suitable technological option for high temperature waste heat recovery in engine power plants[4] and in large ships [5]. Bombarda et al. [4] evaluated that approximately 10 % increase in power output in large-scale diesel engine systems can be achieved by converting exhaust heat into electricity by using Kalina cycle or ORC. Uusitalo et al. [6] investigated the recovery of high temperature waste heat in large-scale gas fired engines by using ORCs and it was estimated that the waste heat recovery system was capable to produce about 10 % increase in the power plant power output. One of the most important steps in designing a waste heat recovery is the selection of working fluid. Uusitalo et al. [7] investigated the use of different hydrocarbons, siloxanes, and fluorocarbons in ORCs. In general, fluids with relatively high critical temperature (in a range from 250 to 350 ^{o}C), such as siloxanes with heavy molecules and high critical temperature hydrocarbons were considered as the most potential candidates for high temperature applications when considering the power output and cycle efficiency. Lai et al. [8] investigated the use of different fluids including alkanes, aromates and linear siloxanes in high temperature ORCs. They evaluated cyclic hydrocarbon cyclopentane as the most suitable fluid candidate for about 300 ^{o}C heat carrier temperature level by taking into account several evaluation criteria. Fernandez et al.[9] investigated the use of different siloxanes in high temperature ORC applications and they concluded that the simple linear siloxanes MDM and MM represent high system performance and also ensure fluid thermal stability. Branchini et al. [10] suggested the use different performance indexes including cycle power output, expansion ratio, mass flow rate ratio, and heat exchange surface for evaluating the most suitable working fluid for the considered heat recovery application. The working fluid not only have an effect on the cycle performance but it has also a significant impact on the sizing and suitable technological solutions for the process main components and cycle layout[11]. It has been also shown that there is significant potential for increasing the cycle power output of WHR systems by adopting supercritical fluid conditions. Schuster et al. carried out an optimization for a supercritical ORC and identified more than 8 % increase in system efficiency when compared to subcritical process[12]. Supercritical fluid conditions for a WHR ORC were also studied by Gao et al. [13]. They concluded that the turbine inlet pressure and temperature highly affects not only the cycle performance but also the turbomachinery size.

Alongside with the use of different types of ORC and Rankine cycles, the use of supercritical Brayton cycles(SBC) have been considered and investigated for various applications in the recent times. When comparing the operational principles of SBC and ORC or other Rankine technologies, the main difference is that in a SBC the working fluid remains at supercritical conditions thorough the whole cycle and the fluid is compressed with a compressor instead of a pump. Unlike in the high temperature ORCs, the use of low critical temperature fluids are preferred instead of high critical temperature fluids in SBCs. Especially, SBC systems using CO_2 as the working fluid have been studied and developed intensively, although no commercial products are yet available based on this technology. The main advantages of using supercritical CO_2 as the working fluid are the high thermodynamic efficiency, high stability at high temperatures, non-toxicity and non-flammability of the working fluid as well as the high power density, which results in reduced component sizes when compared to other type of power cycles[14]. The most potential applications for supercritical CO_2 cycles have been identified to be concentrating solar power plants[15] and future nuclear reactors[16]. Ahn et al. [17] and Li et al. [18] reviewed the literature related to the current research and development of supercritical CO_2 cycles. In both papers it was recognized that there are 12 different cycle layouts that have been proposed and investigated in the literature, ranging from a simple regenerative cycle to more complex cycles with several turbomachines and heat exchangers installed at different parts of the process. Al-Sulaiman and Atif[19] studied different cycle layouts for supercritical Brayton cycles utilizing solar energy. Their results showed that out of different cycle layouts, the highest power outputs were reached with a recompression cycle, in where the flow is splitted and the compression is divided into two stages. In their study, the simple regenerative cycle represented also high cycle efficiencies for the studied application. The use of supercritical CO_2 in waste heat recovery applications has been also considered and investigated. Chen at al. [20] compared the use of a transcritical CO_2 cycle and ORC using R134a as the working fluid for recovering low temperature (about 150 ^{o}C) waste heat. Their results indicated that slightly higher power output could be reached when using CO_2 cycle and that the system using CO_2 as the working fluid is more compact, when compared to the studied ORC system. More recently, system using supercritical CO_2 as the working fluid for recovering exhaust heat of marine gas turbines was investigated[21]. The results showed significant increase potential in the ship energy system thermal efficiency at both full-load and part-load operational conditions. Wang and Dai [22] studied the waste heat recovery potential by using transcritical CO_2 and ORC cycles for recovering waste heat recovery from the cooling energy of recompression supercritical CO_2 cycle. They concluded that the second law efficiencies of these two WHR technologies were comparable.

The high performance of the turbomachines is important for reaching high efficiency for a SBC system. In [23], it was estimated that the turbomachines operating with supercritical CO_2 have compact size and can reach over 90 % efficiency. Similar conclusions were also given related to the compressor design in[24] regarding large scale power systems operating with supercritical CO_2. Conboy et al. [25] concluded based on results from a small scale experimental setup that despite the turbine and compressor are performing reasonably well there are significant heat losses and losses due to fricitional drag when the size of the turbogenerator is small, but these losses can be significantly reduced in the future commercial-scale SBCs. It has been also shown that there are high variations in the fluid properties near the critical point and near the pseudocritical line which affects especially on the compressor design for such a system. In [26] the use of a water pump derived compressor was investigated for compressing supercritical CO_2 as the density of the fluid is high and the fluid is nearly incompressible close to the critical point. Lee et al. [27] investigated experimentally operation of a compressor with supercritical CO_2 and concluded that very high uncertainty on performance measurement was observed due to the high property variations near the critical point. An example on the variation in isobaric specific heat near the critical point is presented for CO_2 in Fig. 1.

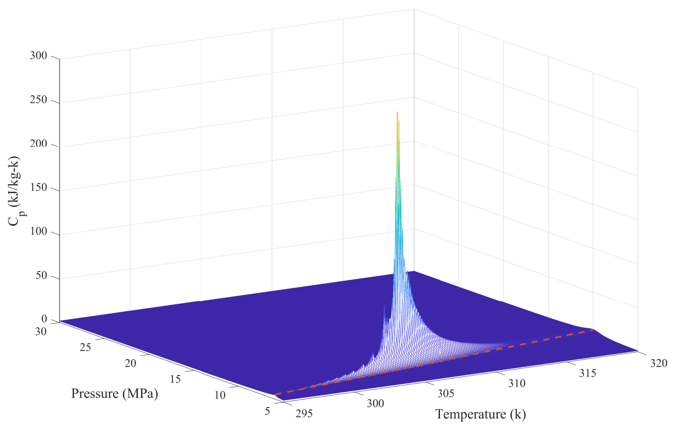

Figure 1: Variation in the fluid isobaric specific heat near the critical point and pseudocritical line. The pseudocritical line is illustrated as dashed line.

In principle, supercritical Brayton cycles could employ a variety of different low critical temperature fluids as their working fluid. Unlike in the field of ORC research, only few studies have been considering the use of some other fluids than CO_2 in SBCs. In [23] several potential fluid candidates were listed and discussed, but no further thermodynamic analysis was carried out with these different fluids. Rovira et al. [28] investigated the factors affecting the performance and design of supercritical Brayton cycles. They concluded that if the ratio of heat source temperature and heat sink temperature is moderate or low, the cycle specific work notably increases if the gas compression begins close the critical point conditions. They also considered other fluids alongside with CO_2 as potential fluid candidates, namely xenon, R41, Ethane, R410a, and R13 but no further analysis was carried out. In addition, closed Brayton cycles using mixtures of carbon dioxide and hydrocarbons have been identified and proposed to be a potential solutions for increasing the cycle efficiency and power output[29]. In addition, Jeong et al. [30] studied the possibility to increase the efficiency of SBC by mixing different fluids with CO_2. The studied fluids were nitrogen (N_2), oxygen (O_2), helium, and argon and they concluded that the highest system efficiency was reached by usign a mixture of CO_2 and Helium. The system efficiency was observed to decrease with the other studied fluids when compared to the cycle efficiency when using pure CO_2.

The literature review shows that different technologies for recovering exhaust heat and converting it into electricity have been intensively studied in the recent years and most of the research efforts have been concentrating on the development of ORC technology, especially at the low power or temperature levels. The previous studies on using SBCs in different applications have shown great potential related to this technology, especially, due to the high cycle efficiencies and compact sizes of the process components. However, the potential of using supercritical Brayton cycles for recovering high temperature waste heat from large scale engines has not been investigated and identified. The scientific novelty and the main objectives of this research is to investigate and evaluate the power production potential from high temperature exhaust heat of a large-scale engine by using closed Brayton cycles adopting supercritical fluids. As the previous research and development work of SBCs has been mainly concentrating on systems having significantly high temperatures, large power scale, and using CO_2 as the working fluid, an interesting research question arises on could some other low critical temperature fluid be more suitable and effective choice for this type of energy conversion cycles instead of CO_2. The system is thus, studied by using different low critical temperature fluid candidates and the main operational parameters affecting on the cycle power output are investigated and highlighted. In addition, as the literature review also showed that the system efficiency is highly dependent on the turbomachines performance and design, the results of centrifugal compressor and radial turbine design analysis, as well as turbine loss evaluation with different fluids and operational parameters are presented and discussed in this paper.

2. Cycle configurations and numerical methods

A simple recuperated cycle configuration as well as an intercooled and recuperated cycle configuration were selected for the SBC analysis. In the studied cycles the working fluid is at supercritical state thorough the process and recuperator is included in studied cycle layouts for preheating the fluid entering the heater. Similar simple cycle configuration has been used for example in the experimental facility presented in[31] and in the intercooled cycle a second compressor and intercooler have been added between the compressor stages. The main components of the studied cycles as well as the simplified process diagrams are presented in Fig. 3a and b. It should be noted that also several other cycle configurations have been proposed in the literature(e.g. in[17, 18]) for SBCs, representing improvements in the cycle efficiency, especially when operating at very high temperatures. However, the temperature and power level adopted in this study are rather low, following that the use of more complex cycle architectures were not considered. For example the recompression cycle allowing to maximize the heat transfer in system recuperators, was not considered in this study as it was observed that in this application the cycle performance is not as sensitive on the heat transfer in the recuperator as it is in higher temperature applications (results presented and discussed in Fig. 7a and b). In addition, the cycle configurations selected for this study are well comparable in terms of complexity to the typical WHR ORC systems.

The SBC simulations were carried out by using four different fluids that were selected and evaluated as the most suitable fluid candidates among the considered fluids. The selection of the fluid candidates was based mainly on the critical temperature of the fluid that has to be slightly below or close to the studied compressor inlet temperatures. This ensures supercritical fluid state thorough the cycle and allows to reach high cycle performance under the studied conditions. The studied fluids are namely, carbon dioxide (CO_2), ethane, ethylene, and hexafluoroethane (R116). The molecular formula, molecular weight, critical properties and flammability of the studied fluids are summarized in Table 1. In addition to the studied fluids, sulfur hexafluoride was also evaluated as suitable candidate for the studied system, but due to the insufficient thermodynamic data for calculating the turbine losses available in [32], this fluid was not included in the final analysis presented in this paper.

The exhaust gas temperature of 354 ^{o}C and exhaust gas flow rate of 30.2 kg/s were used in the analysis as the heat source input values. The studied exhaust gas temperature level and flow rate were selected based on the exhaust values of a modern 4-stroke gas fired engine, having the power output of 18.3 MW[33]. The exhaust gas thermal energy was assumed to be wasted in the engine system without a heat recovery, meaning that there is no usage for the heat power and the target is to maximize the electricity production of the studied engine system. Thus, the conversion of exhaust gas heat into electricity is assumed to directly increase the from fuel to usable energy efficiency. It was also assumed that the studied WHR system has no effect on the gas engine performance.

Table 1: Properties of the studied working fluids.

Fluid	Molecular formula	M, [kg/kmol]	T_{crit}, [^oC]	p_{crit}, [bar]	flammability
Carbon dioxide	CO_2	44.0	30.95	73.8	non-flammable
Ethane	C_2H_6	30.1	32.15	48.7	flammable
Ethylene	C_2H_4	28.1	9.15	50.42	flammable
Hexafluoroethane (R116)	C_2F_6	138.0	19.85	30.5	non-flammable

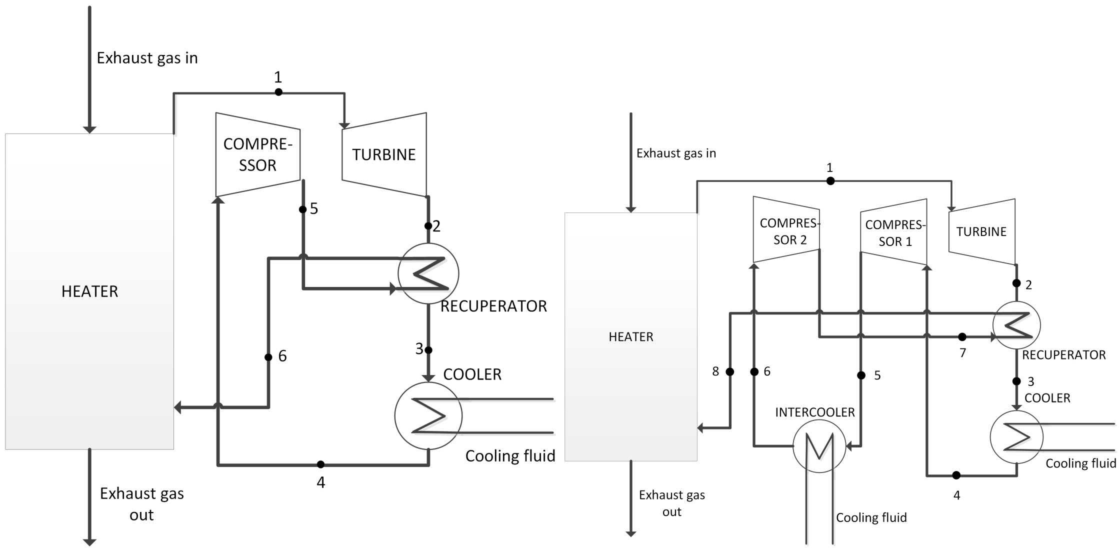

(a) (b)

Figure 2: Simplified process diagrams of the studied recuperated simple SBC and intercooled SBC.

2.1. Cycle analysis

The process simulations were carried out by using a cycle analysis tool developed at Lappeenranta University of Technology capable for analyzing closed Brayton cycles. The calculation is based on the general calculation principles of closed Brayton cycles and the fluid thermodynamic state at the each process node was defined by using a commercial thermodynamic library Refprop[32] containing accurate properties and equations of states for the studied fluids. The energy and continuity equation were solved at the inlet and outlet of each process component based on the given input parameters. The thermodynamic cycle model uses the working fluid, component efficiencies, turbine inlet state, compressor inlet state and the heat source values as the input parameters and solves the unknown properties at different process nodes. No pressure or heat losses in the system piping and in the heat exchangers were included in order to simplify the analysis.

The main equations used in the SBC analysis are presented in the following. The heat rate extracted

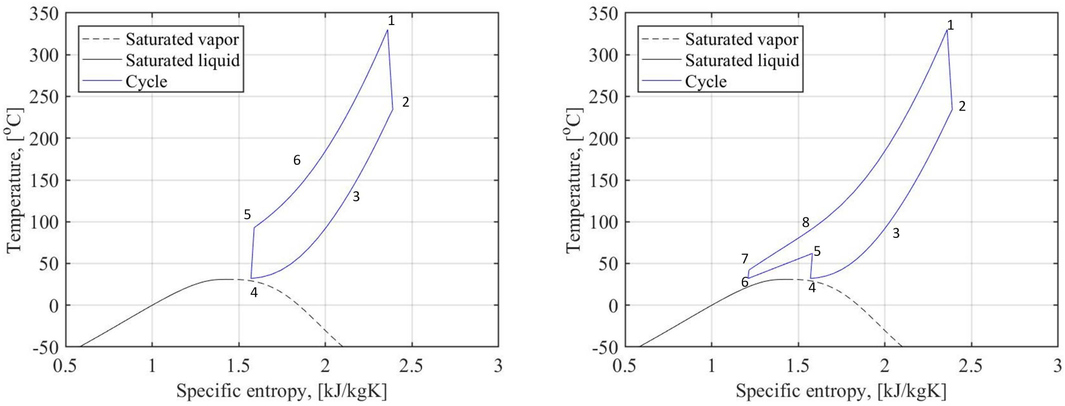

(a) (b)

Figure 3: Example of the studied supercritical Brayton cycles on T-s plane. (a) is for simple cycle and (b) is for intercooled cycle. In both cycles, CO_2 is used as the working fluid and the turbine inlet pressure of 200 bar and the compressor inlet temperature of 32 ^{o}C is used.

from the exhaust gas to the working fluid was solved as,

$$\phi_{\mathrm{h}} = q_{\mathrm{m,eg}} c_{p,eg} (T_{\mathrm{eg,h,in}} - T_{\mathrm{eg,h,out}}). \tag{1}$$

The working fluid mass flow rate was solved by using the energy balance of the heater as

$$q_{\mathrm{m,wf}} = \frac{\phi_{\mathrm{h}}}{(h_{\mathrm{h,out}} - h_{\mathrm{h,in}})}. \tag{2}$$

The turbine outlet enthalpy was solved by using the definition of turbine isentropic efficiency,

$$h_{\mathrm{t,out}} = h_{\mathrm{t,in}} - \eta_{t,s} (h_{\mathrm{t,in}} - h_{\mathrm{t,out,s}}). \tag{3}$$

in which $h_{\mathrm{t,out,s}}$ was solved based on the isentropic expansion from the turbine inlet state to the turbine outlet pressure.

The mechanical power of the turbine was calculated as

$$P_{\mathrm{t}} = q_{\mathrm{m,wf}} (h_{\mathrm{t,in}} - h_{\mathrm{t,out}}). \tag{4}$$

The compressor outlet enthalpy was solved by using the definition of compressor isentropic efficiency,

$$h_{\mathrm{c,out}} = h_{\mathrm{c,in}} + \frac{(h_{\mathrm{c,out,s}} - h_{\mathrm{c,in}})}{\eta_{c,s}}. \tag{5}$$

in which $h_{\mathrm{c,out,s}}$ was solved based on the isentropic compression from the compressor inlet state to the compressor outlet pressure.

The mechanical power of the compressor was calculated as

$$P_{\mathrm{c}} = q_{\mathrm{m,wf}}(h_{\mathrm{c,out}} - h_{\mathrm{c,in}}). \tag{6}$$

The electric power output of SBC was calculated as,

$$P_{\mathrm{e}} = \eta_g (P_{\mathrm{t}} - P_{\mathrm{c}}). \tag{7}$$

The recuperator effectiveness defining the temperature change in the recuperator was used for calculating the fluid temperature at the recuperator hot side outlet. The recuperator effectiveness was defined as,

$$\varepsilon = \frac{(T_{\mathrm{hot,in}} - T_{\mathrm{hot,out}})}{(T_{\mathrm{hot,in}} - T_{\mathrm{cold,in}})}. \tag{8}$$

The cold side outlet state was solved from the energy balance of the recuperator. The cycle efficiency is determined by using the net electric power output from the system and the heat power that is extracted from the exhaust gases to the working fluid in the heater.

$$\eta_{\mathrm{e}} = \frac{P_{\mathrm{e}}}{\phi_{\mathrm{h}}}. \tag{9}$$

The main parameters that were used in the cycle analysis are summarized in Table2. The exhaust gas temperature at the heater outlet was varied depending on the cycle operational conditions by following the criteria that the temperature difference between the exhaust gas and working fluid does not exceed the minimum limit of 20 ^{o}C at the cold end of the heater. The maximum temperature at the cycle side has been selected based on the temperature level of the exhaust gases and it has been used for all the studied fluids in order to evaluate the thermodynamic cycles in a comprehensive way. It should be noted, that the selected maximum turbine inlet temperatures above 300 ^{o}C can be close to the thermal stability threshold with some organic fluids[34]. The maximum pressure in the cycle of 400 bar was adopted in the cycle analysis and the simulations were carried out by using different turbine inlet pressures in order to investigate the effect of cycle pressure level on the cycle performance and turbomachinery design. However, it should be noted that the highest studied pressure levels are significantly higher when compared to the more conventional power systems and the very high pressure level could lead to difficulties in material strength and sealing of the system. The compressor inlet pressure of 0,5 bar higher than the critical pressure of the fluid was used and critical temperature slightly higher than the critical temperature of the fluid were used in the simulations, in order to ensure supercritical fluid conditions at the compressor inlet. According to Angelino and Invernizzi[35] this type of cycle reaches the highest performance when the compressor inlet condition is close to the critical point of the fluid. The validation of the cycle analysis code is presented in Section *Cycle and turbomachinery code validation.*

Table 2: Process simulation parameters.

Cooler outlet temperature/compressor inlet temperature	30,50, [^{o}C]
Generator efficiency	95, [%]
Exhaust gas temperature	354, [^{o}C]
Exhaust mass flow rate	30.2, [kg/s]
Minimum temperature difference in the heater	20, [^{o}C]
Maximum turbine inlet temperature	330, [^{o}C]
Maximum turbine inlet pressure	400, [bar]
Compressor inlet pressure	p_{crit} + 0.5, [bar]

3. Turbine and compressor design analysis

The turbine type for the analysis was selected to be a radial turbine and compressor type was selected to be a centrifugal compressor as this type of turbomachines have simple structure and can reach high efficiency in small-capacity applications. Radial turbines have been used for example in an experimental system for supercritical CO_2[36, 37] and this type of turbines are also widely used in ORC applications e.g.[38, 39]. Centrifugal compressors have been considered in several studies for compressing supercritical CO_2 and has been also used in experimental facilities[40]. Examples of a radial turbine and centrifugal compressor rotor geometries are shown in Fig. 4a and b.

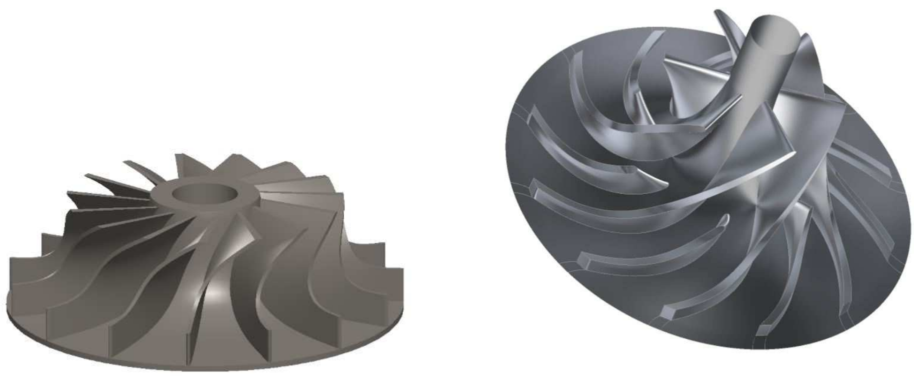

(a) (b)

Figure 4: Examples of radial turbine (a) and centrifugal compressor (b) geometries.

The turbomachinery design is based on the design principles presented by Balje[41] and Rohlik[42]. The suitable turbine rotational speed was calculated by setting the specific speed N_s as an input value in the analysis and by using the working fluid flow rate and isentropic enthalpy change that were solved in the cycle design analysis. The specific speed can be defined as

$$N_s = \frac{\omega {q_{v2}}^{0.5}}{{\Delta h_s}^{0.75}}. \tag{10}$$

The rotational speed was calculated by using $N_s = 0.6$ which is close to the optimal value for radial turbines, which is about 0.4 - 0.8 according to the design guidelines [41, 42]. The same equation can be used for compressors for defining the specific speed but in this case, the volumetric flow rate at the compressor rotor inlet is used.

The turbine design is based on solving the suitable geometry by using velocity triangles consisting of three vectors, namely the absolute velocity c, peripheral velocity u and relative velocity w. A schematic example shape of a velocity triangle at the turbine rotor inlet is presented in Fig.5. The expansion was divided equally for turbine stator and rotor. For the turbine stator, efficiency of 90 % was used for estimating the enthalpy at the stator outlet. The enthalpy at the stator outlet was calculated as,

$$h_1 = h_0 - \eta_{st}(h_0 - h_1 s). \tag{11}$$

and the absolute flow velocity c_1 at the stator outlet was calculated by using the stator inlet and outlet enthalpy

$$c_1 = \sqrt{2(h_0 - h_1)}. \tag{12}$$

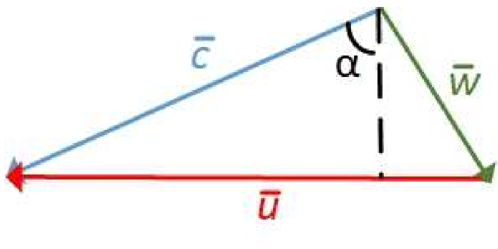

Figure 5: A schematic example of velocity triangle at the rotor inlet.

The optimal absolute flow angle α at the rotor inlet was selected as a function of the specific speed by following the principles presented in[42]. The velocities at the rotor inlet u_1 and c_{u1} are solved by using the absolute flow angle and the total enthalpy change over the turbine. The tangential component of the absolute velocity c_{u1} was solved from the rotor inlet velocity triangle and the peripheral velocity u_1 was solved by using the Euler turbomachinery equation in where the rotor discharge flow was assumed to be axial,

$$u_1 = \frac{\Delta h_t}{c_{u1}} \tag{13}$$

The turbine diameter can be calculated as,

$$d_1 = \frac{u_1}{\pi n} \tag{14}$$

The rotor inlet blade height was calculated by using the continuity equation. The rotor diameter and blade height at the rotor outlet are calculated by using the diameter ratios d_{2tip}/d_1 and d_{2hub}/d_{2tip} that were defined by following the guidelines of Rohlik[42].

In the turbine loss analysis the stator loss, rotor passage loss, and the disk friction loss were calculated for each turbine design. The turbine rotor disk friction loss and passage loss were evaluated according to Daily and Nece [43] and Balje [44]. These models were selected for the study as similar loss correlations have been previously used for estimating turbomachinery losses for radial turbines operating with supercritical CO_2[45]. The disk friction loss was evaluated by using the following equations

$$\Delta h_{df} = 0.5 f(\rho_1 + \rho_2) D_1^2 \frac{u_1^3}{16 q_{m,wf}} \tag{15}$$

in where,

$$Re = \rho_1 u_1 \frac{D_1}{2\mu_1} \tag{16}$$

$$f = \frac{0.0622}{Re^{0.2}} \tag{17}$$

.

The rotor passage loss was evaluated by using the following equation

$$\Delta h_{pass} = \varphi^{1.75} \frac{(1+\kappa)^2}{8} \varsigma u_1^2 \tag{18}$$

in where,

$$\varsigma = 0.88 - 0.5\varphi \tag{19}$$

$$\kappa = \frac{c_{r1}}{c_{r2}} \tag{20}$$

$$\varphi = \frac{c_{r1}}{u_1} \tag{21}$$

The total loss in the turbine is defined as

$$\Delta h_{loss} = \Delta h_{df} + \Delta h_{pass} + \Delta h_{stator} \tag{22}$$

and the turbine efficiency is defined as

$$\eta_t = \frac{\Delta h_s - \Delta h_{loss}}{\Delta h_s} \tag{23}$$

The incidence loss was not taken into account in the analysis since only different turbine design points were studied and zero incidence for the flow at rotor inlet was assumed at the design condition. In addition, tip clearance loss was not included since there is only little information in the literature on the suitable loss correlations and methods for accurately calculating the tip clearance loss for radial turbines, especially with non-conventional and supercritical working fluids. Thus, the results presented in this study can slightly overestimate the turbine isentropic efficiency, especially with turbines having small blade heights at the rotor inlet. However, in the experimental work by Dambach et al. [46] it was concluded that the tip clearance loss with radial turbines is less significant when compared to axial turbines. The radial turbine design code and predicted losses were compared and validated against radial turbine designs available in the literature and this validation and comparison is presented in the following section.

A simplified compressor design was also included in the analysis to evaluate the compressor size and geometry for the studied system. The compressor geometry was calculated for different fluids and operational conditions by using the Sandia Laboratory experimental setup main compressor[40] as the reference compressor design. The compressor geometry analysis was carried out only for the simple cycle configuration with different fluids in order to limit the number of the studied cases. However, the compressor design for the intercooled cycle was included for CO_2 in order to compare the compressor design in simple and intercooled cycle. The compressor loss calculations were not included in the analysis. The working fluid flow rate and compressor inlet and outlet conditions were used as the input values for defining the compressor geometry. In addition, the compressor rotational speed was set to equal value as were gained in the turbine design for the respective conditions as the turbine and compressor were assumed to be assembled on the same shaft. This resulted in compressor specific speeds in the range of 0.6-1.0 in the simple cycle layout that can be considered to be in a feasible range for centrifugal type compressors[41]. In the design, the shape of the velocity triangle at the compressor wheel outlet was defined by giving the velocity ratios $c_{r1'}/u_{1'}$ and $c_{u'_1}/u'_1$ as well as diameter ratios $d_{0'tip}/d_{1'}$ and $d_{0'hub}/d_{1'tip}$ as inputs. These ratios were defined and selected based on the reference compressor design[40] and were kept constant thorough the study for different fluids and operational conditions. The compressor diameter and blade height at the impeller inlet and outlet were solved by using the same methods as were applied and described for the turbine design.

3.1. Cycle and turbomachinery code validation

SBC cycle model was validated against data available in the literature. For the cycle code validation, the simulation results of a transcritical CO_2 cycle presented by Kim et al. [47] were used as the reference case. The turbine inlet pressure and temperature, outlet pressure, isentropic efficiency, and recuperator effectiveness were set to the same values as were used in[47]. The main results of this comparison are presented in Table 3 for the simple cycle configuration. The fluid compression calculation was validated and compared against the design values of the main compressor of the Sandia laboratory experimental setup[36]. The results of the comparison are presented in Table 4. In this comparison, the fluid state at the compressor inlet, compressor outlet pressure, fluid mass flow rate and compressor efficiency were set to the equal values as in the reference[36].

Table 3: Cycle code validation.

	ΔT [K]	ΔT [K] [47]	Δh [kJ/kg]	Δh [kJ/kg] [47]
Expansion	151.0	151.0	169.9	169.9
Cooler	33.6	34.2	221.5	222.7
Heater	301.6	302.5	371.9	373.1
Recuperator hot side	395.5	394.7	450.1	449.0
Recuperator cold side	259.2	258.3	450.1	449

Table 4: Compressor calculation validation.

	P [kW]	ΔT [K]
Sandia main compressor	49	17.8
Sandia main compressor [36]	51	19.0
dev	2	1.2

The turbine design code was validated and the results are compared against different radial turbine designs for non-conventional working fluids available in the literature. The design comparison is carried out for three different radial turbine designs using siloxane MDM, CO_2 at supercritical state and R245fa as the working fluids. In the comparison presented in Table 5, the turbine inlet temperature and pressure, outlet pressure, and fluid flow rate were set to the same values as in the literature references. In addition, the turbine design specific speed, absolute flow angle α_1, flow acceleration in the turbine stator, and the degree of reaction, were set to the same values as were presented in the references if this information was available. If the information was not given in the references, these values were selected in order to have the turbine design results as close as possible to the turbine values presented in the references. Turbine wheel dimensions, rotational speed, power output, and efficiency were calculated by using the developed turbine design code and the results were compared against the turbine dimensions and performance given in the literature references.

Table 5: Comparison of the turbine design code results and the turbine dimensions and performances available in the literature.

	fluid	D_{rot}, [mm]	n_{rot}, [rpm]	P_t [kW]	η_t [%]	N_s -	α [deg]
[39]	R245fa	$\approx$ 125	20 000	32.7 (electrical)	82 (max)	-	-
Turbine design code	R245fa	136.3	21 788	36.0 (mechanical)	86.5	0.45	72
Dev %	-	9.04	8.94	-	5.5	-	-
[48]	MDM	144	31 455	13.0	76	0.49	69.4
Turbine design code	MDM	146.0	31 348	12.6	79.5	0.44	69.4
Dev %	-	1.4	-0.3	-2.8	4.6	-	-
[36, 37]	CO_2	67.6	75 000	178	87	-	-
Turbine design code	CO_2	66.2	75 474	176.7	86.2	0.36	75
Dev %	-	-2.1	0.6	-0.7	-0.9	-	-

The comparison shows that the obtained results are well in line with the used turbine design references, especially when considering the turbine diameter and rotational speed. Some deviations can be observed in the predicted turbine isentropic efficiencies, and power outputs with all the turbines. The smallest deviations were found for the turbine operating with supercritical CO_2 and the highest deviations in the power output and efficiency predictions were observed with the turbines operating with MDM and R245fa. However, the maximum deviations of less than 10 % were obtained for all the studied parameters. Overall it can be concluded that the applied turbine design method can be considered to be suitable for qualitative and preliminary evaluation on the effect of using different fluids and cycle operating conditions on turbine efficiency and geometry, as the same method is systematically implemented for the radial turbine design with all the studied fluids and conditions thorough the analysis. Overall, the validation of both the cycle and turbine design codes show good agreement when compared to the selected literature references.

The validation of the compressor design code is presented in Table 6. The flow rate through the compressor, compressor inlet and outlet state, and the design rotational speed were set to the equal values as were used in[40]. In general, the designed compressor wheel has diameters and blade height close to the values of the reference compressor. The deviation in the impeller outlet blade height was 0.3 mm and the maximum deviation out of the studied diameters was 0.5 mm.

Table 6: Comparison of the compressor design code results and the centrifugal compressor design available in the literature.

	fluid	$D_{1'}$, [mm]	$D_{0'hub}$, [mm]	$D_{0'tip}$ [mm]	$b_{1'}$ [mm]
[40]	CO_2	37.4	18.7	5.1	6.8
Compressor design code	CO_2	37.2	18.6	5.6	6.5

4. Results and Discussion

In this section the main results of the study are presented. First, a sensitivity analysis on different process parameters is carried out by using CO_2 as the working fluid. Second, the results of the effect of different fluids and operational parameters on the power production potential and efficiency are presented and discussed. In this thermodynamic analysis, the turbomachinery isentropic efficiencies are kept constant for all the fluids and operational parameters. Third, the design and loss evaluation on the process radial turbine and centrifugal compressor with different fluids and operational conditions are presented and discussed.

4.1. Sensitivity analysis of main process parameters with CO_2

The sensitivity of the cycle performance on the main process parameters were studied first with CO_2 as the working fluid. The studied parameters are the compressor and turbine efficiency, turbine inlet temperature and the recuperator effectiveness. The results presented in the following were obtained by using the simple cycle configuration and compressor inlet temperature of 50 ^{o}C. The turbine inlet pressure was varied between 100 bar to 400 bar and the turbine inlet temperature was varied from 270 ^{o}C to 330 ^{o}C in the analysis. The results of the effect of turbomachinery efficiency on compressor power consumption and turbine power output are presented in Figure 6a and b. The compressor power consumption was calculated for a single compressor without intercooling. The result of the sensitivity of turbine inlet temperature on the cycle performance is presented in Figure6c. In these simulations turbomachinery efficiencies of 85% were adopted.

The results show that the compressor power consumption and turbine power output are highly sensitive on the efficiency of the turbomachines. The effect of the turbine or compressor efficiency are more pronounced as the turbine inlet pressure is high, when compared to a cycle designed for lower pressure ratio. Thus, for achieving a high efficiency and net power output for the studied system, it is of high importance that both the compressor and turbine can be operated with high efficiency. The results of the effect of turbine inlet temperature show that the higher the turbine inlet temperature, the higher the cycle power output. Thus the turbine inlet temperature of 330 ^{o}C was used in the following analysis which is 24 ^{o}C less than

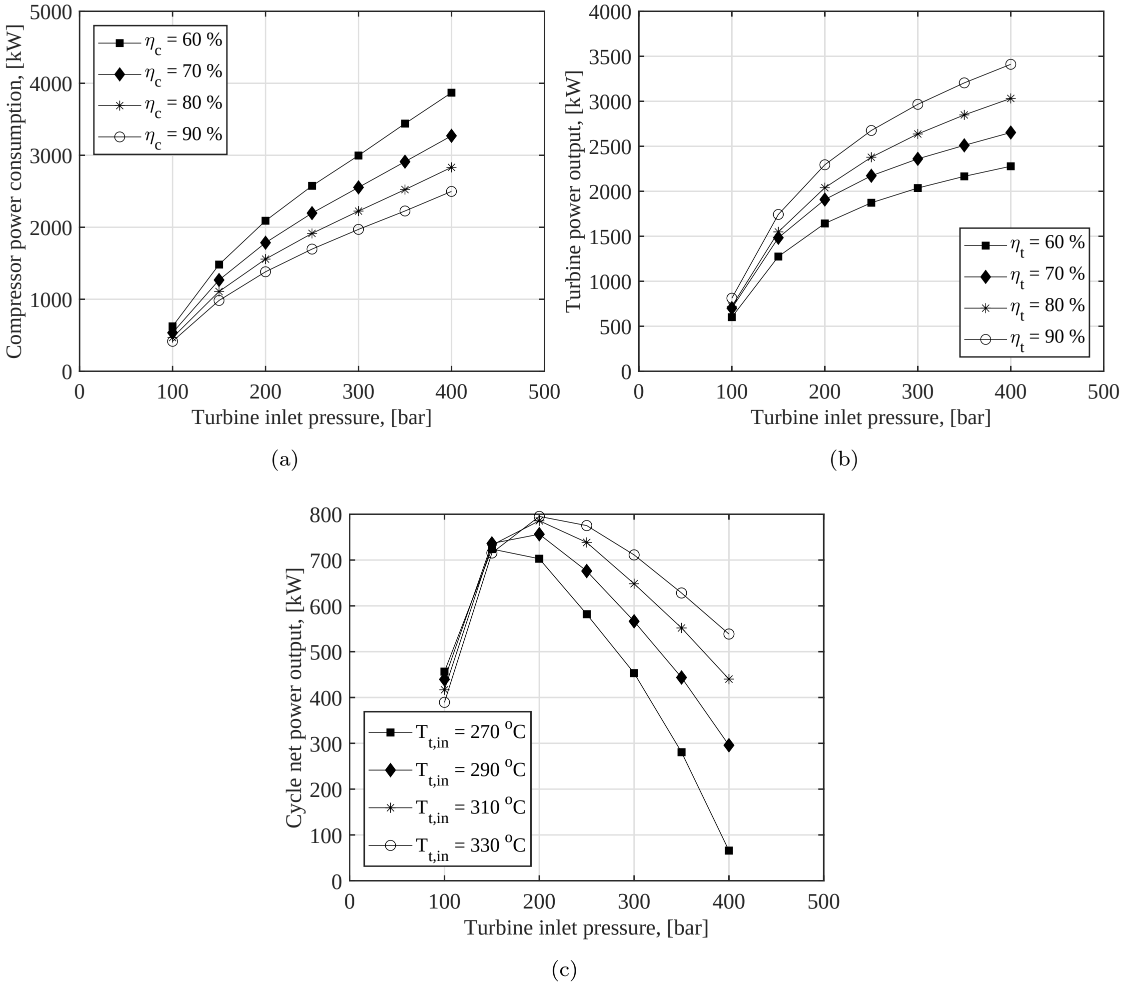

Figure 6: Effect of compressor efficiency on compressor power consumption (a), turbine efficiency on turbine power output (b), and turbine inlet temperature on cycle net power output (c).

the temperature level of the exhaust gases. This was estimated to ensure sufficient temperature difference between the heat source and working fluid at the hot end of the heater.

The sensitivity of recuperator effectiveness on the cycle power output and the effect of the recuperator effectiveness on the heat source temperature at the heater outlet are presented in Figures 7a and b. The analysis on the effect of recuperator effectiveness on power output show that the recuperator effectiveness has only minor effect on the cycle power output with the applied method. This can be explained that in the cycle analysis the heat source temperature at the heater outlet was defined by using the minimum temperature difference between the heat source and working fluid. Thus, as the recuperator effectiveness is increased the heat source temperature at the heater outlet has to be also increased in order to maintain the required temperature difference between the heat source and the working fluid. This results in a lower heat rate in the heater but increases the amount of heat transferred in the recuperator. Thus, it was concluded that the benefit of using a high recuperator effectiveness in the cycle is not as significant in this application, as have been presented in the literature for higher temperature applications.

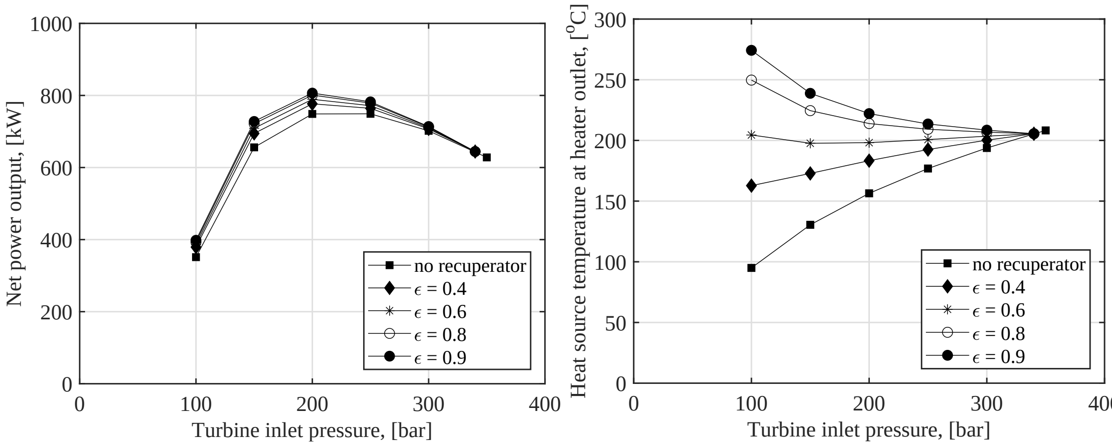

(a) (b)

Figure 7: Effect of recuperator effectiveness on cycle net power output (a) and heat source temperature at the heater outlet(b).

In addition to the above presented results, the effect of the pressure level between the Compressor 1 and Compressor 2 on the intercooled cycle performance was studied by using CO_2 as the working fluid. The pressure rise in the compressor 1 was defined as

$$p_{comp1,out} = x(p_{comp1,in} * p_{comp2,out})^{0.5} \tag{24}$$

and the results obtained for different x values are presented in Fig.8a and b. Based on the obtained results, the pressure level between the Compressor 1 and Compressor 2 has an effect on the cycle power output, especially when using the higher CIT of 50 ^{o}C. For both studied cases a higher cycle power output was reached when the Compressor 1 pressure ratio is lower when compared to the pressure ratio of the Compressor 2. However, by designing the pressure ratio of both compressors to be equal (x = 1), the power as well as the wheel dimensions of Compressor 1 and Compressor 2 are in the same order of magnitude that was considered as beneficial for the turbomachinery design for such a system. Thus, x = 1 was used in the intercooled cycle analysis in the following.

4.2. Results of the cycle analysis

The results of the cycle analysis for the simple cycle configuration and intercooled cycle configuration are presented in the following. The results were obtained by using turbine and compressor efficiency of 85 % that were selected based on previous research works on supercritical CO_2 turbomachinery[23, 17, 36, 47]. The maximum degree of recuperation of 0.7 was used and the simulations were carried out by using compressor

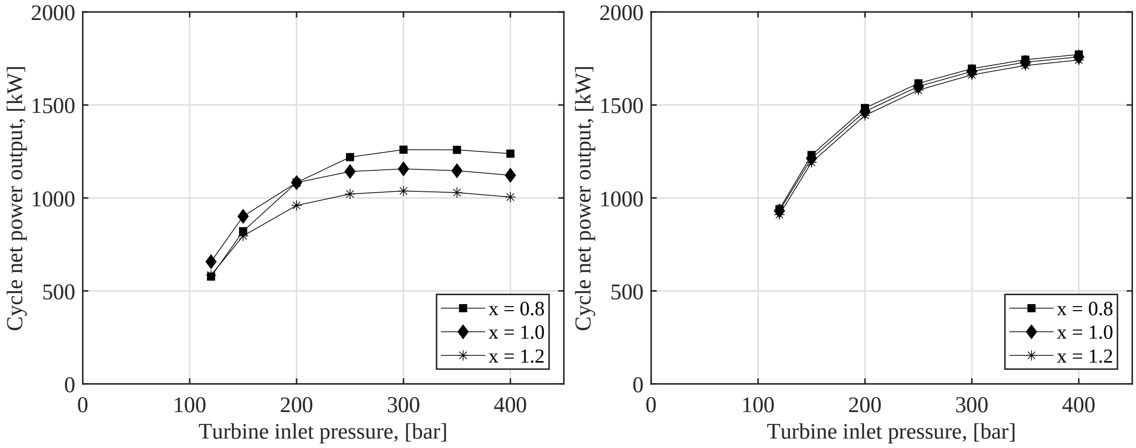

Figure 8: Effect of compressor 1 outlet pressure on the power output of intercooled SBC. Results presented in (a) were obtained by using CIT of 50 ^oC and (b) were obtained by using CIT of 31 ^oC.

inlet temperatures (CIT) of 30 ^oC and 50 ^oC in order to study the effect of the compressor inlet temperature on the cycle performance. With the lower temperature conditions slightly higher temperatures of 31 ^oC and 33 ^oC were used for CO_2 and ethane, respectively, in order to maintain the fluid at supercritical state at the compressor inlet.

The results of the power output are presented in Figures 9a-d and cycle efficiency in Figures 10a-d with different turbine inlet pressures and with different fluids.

The use of CO_2 as the working fluid resulted in higher electric power outputs in all the studied cases when compared to the other fluids and ethane reached the second highest performances. In general, the use of intercooling in the cycle and low compressor inlet temperature results in highest cycle performances. The maximum electric power output of 1759 kW was simulated with CO_2 by using the lower compressor inlet temperature and turbine inlet pressure of 400 bar. The maximum electric power output of 1156 kW was obtained by using the compressor inlet temperature of 50 ^oC and turbine inlet pressure of 300 bar. These values correspond to 9.6 % and 6.3 % of the gas engine power output. This maximum power production potential is slightly lower when compared to the use of ORC technology for recovering exhaust heat of large-scale engines according to the previous studies e.g. [4, 6]. Corresponding maximum power outputs are about 440 kW and about 150 kW lower with ethane when compared to the results with CO_2. The use of ethylene and R116 as the working fluids resulted in lower maximum cycle performances when compared to ethane and CO_2. The turbine inlet pressure, resulting in the highest power output, is dependent on the compressor inlet temperature, cycle configuration and working fluid. With the lower compressor inlet temperature, the highest power outputs were simulated with the highest turbine inlet pressures between 300 bar to 400 bar, with CO_2, ethane and R116. When ethylene is used as the working fluid, the maximum power output was simulated by using a lower turbine inlet pressure close to 200 bar. With the higher

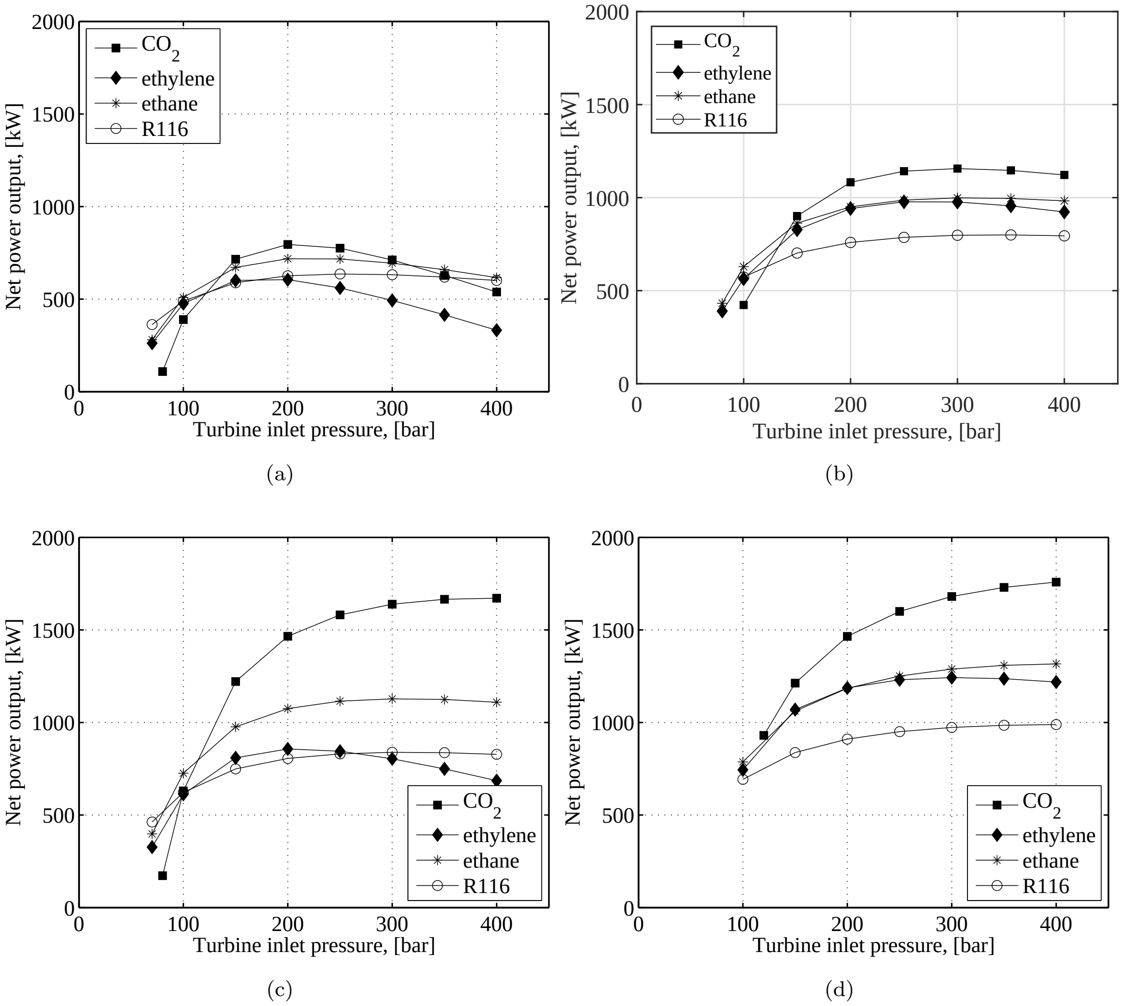

Figure 9: Effect of turbine inlet pressure on SBC power output. Results presented in (a) are for simple cycle and (b) for intercooled cycle with CIT of 50 ^{o}C. Results presented in (c) are for simple cycle and (d) for intercooled cycle with CIT of 30 ^{o}C.

compressor inlet temperature, the turbine inlet pressure resulting in the highest power outputs is lower with all the studied fluids when compared to the cycle with the lower compressor inlet temperature. The maximum cycle efficiencies above 20 % were simulated with CO_2 and ethane by using the lower compressor inlet temperature and high turbine inlet pressure, whereas the maximum cycle efficiencies close to 15 % or slightly above 15 % were simulated for all the studied fluids with the compressor inlet temperatures of 50 ^{o}C. It should be noted that for reaching the low compressor inlet temperature, resulting in the highest performances, a cooling fluid with a low temperature has to be available for the cycle. Thus, to reach the lower compressor inlet temperature is not possible in hot climates and in applications in where cooling fluid temperatures below 30 ^{o}C are not available.

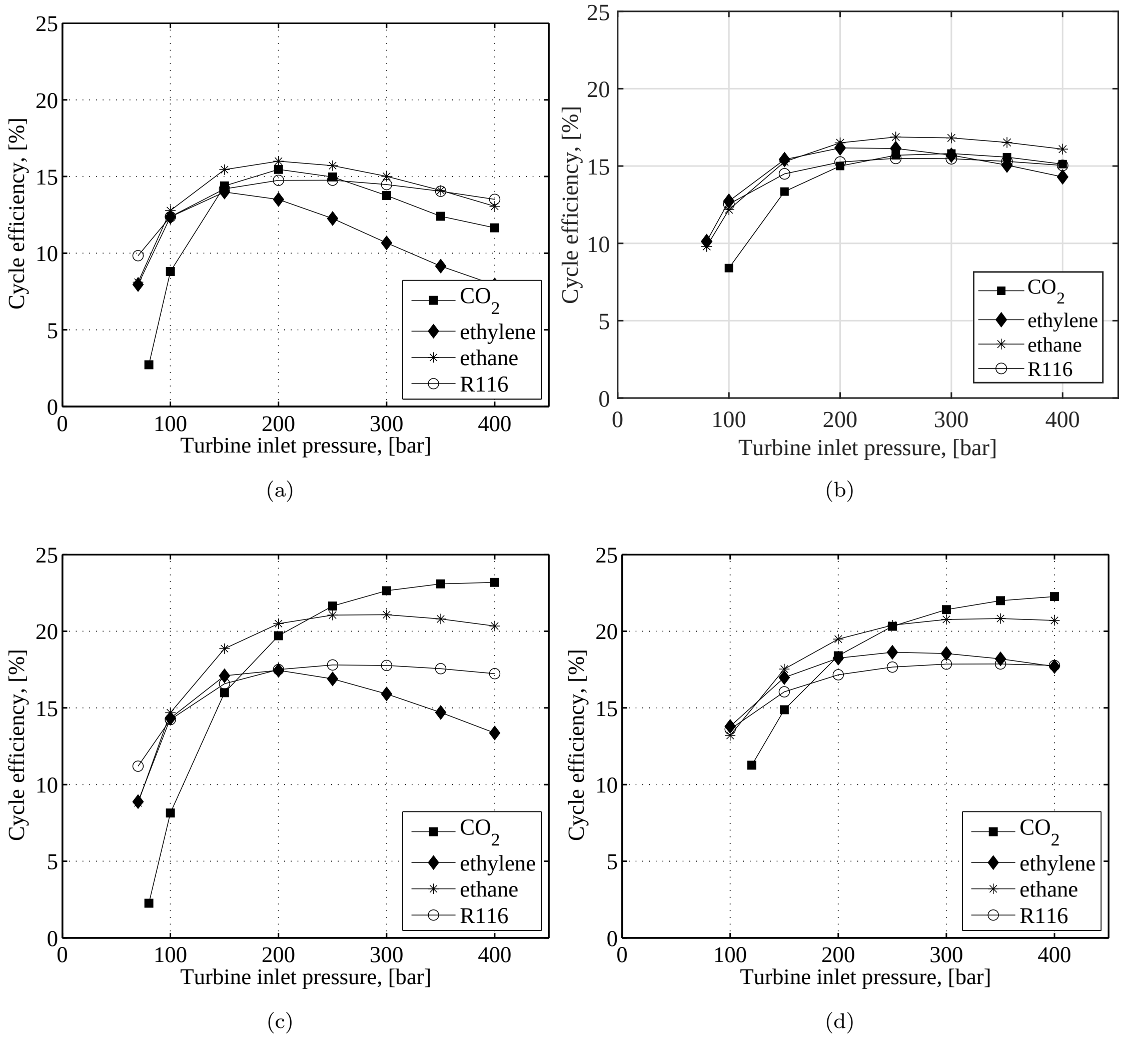

Figure 10: Effect of turbine inlet pressure on SBC efficiency. Results presented in (a) are for simple cycle and (b) for intercooled cycle with CIT of 50 ^{o}C. Results presented in (c) are for simple cycle and (d) for intercooled cycle with CIT of 30 ^{o}C.

The results of the turbine mechanical power output and the power consumption of the fluid compression are presented in Figures 11a-c. These results were obtained by using the lower compressor inlet temperature. The cycle using ethylene as the working fluid results in the highest turbine mechanical power. However, the power consumption of the compressor with this fluid is significantly higher when compared to the other studied fluids. This mainly explains the low cycle power output when using ethylene as the working fluid. CO_2 represents the second highest turbine power and in addition, the power consumption of the compressing the fluid is significantly lower when compared to the other studied fluids, which results in high cycle performances. With all the studied fluids, the intercooling between the compressors reduces the compression power consumption, which mainly explains the higher cycle performances when using the intercooled cycle configuration.

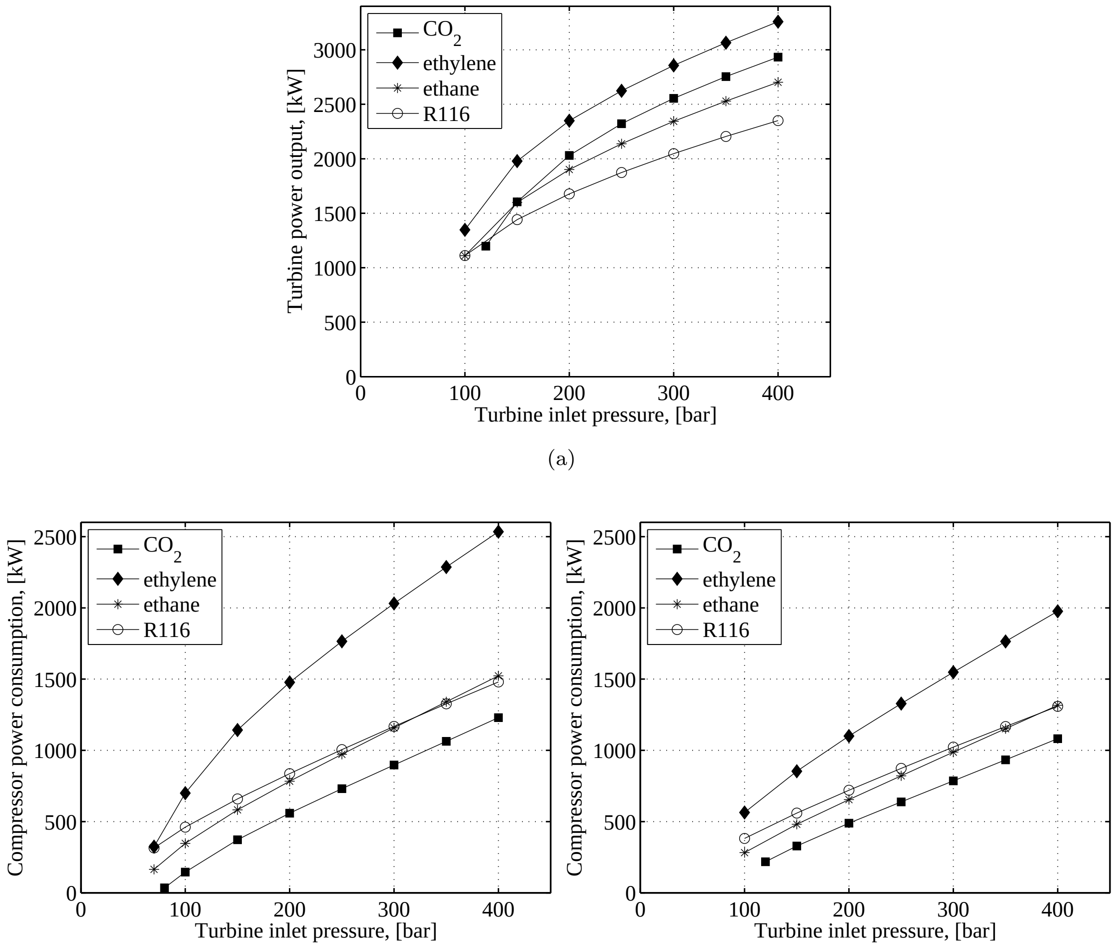

(a)

(b)

(c)

Figure 11: Effect of turbine inlet pressure on turbine power output (a), and compressor power consumption (b) and (c). (b) is for single stage compression and (c) is for the intercooled compression. The simulations were performed by using the lower CIT.

The results of the heater heat rate for the studied cases are presented in Figures 12a-d. Based on the simulation results the system using CO_2 as the working fluid can extract higher amount of heat from the heat source when compared to the other studied fluids, especially in the simple cycle configuration. The differences in the heater heat rates can be explained by the deviations in the working fluid temperatures at the heater cold end with different fluids, cycle configurations, and cycle operating pressures. For example, as presented earlier the use of ethane as the working fluid resulted in comparable or slightly higher cycle efficiencies when compared to the cycles operating with CO_2 but the cycle power outputs were significantly lower because of the lower capability to extract heat from the exhaust gases in the heater. In general, as the turbine inlet pressure increases, higher amount of heat power can be extracted from the heat source in the heater. The high turbine outlet temperature and high heat transfer in the system recuperator can explain the lower heat rate in the heater if a low turbine inlet pressure is adopted. Consequently, this leads to higher exhaust gas temperature at the heater outlet and reduces the heater heat rate, when compared to the cycles adopting higher pressure ratio over the turbomachines. The use of intercooling and low compressor inlet temperature increases the amount of heat that can be transfered from the exhaust gases to the working fluid.

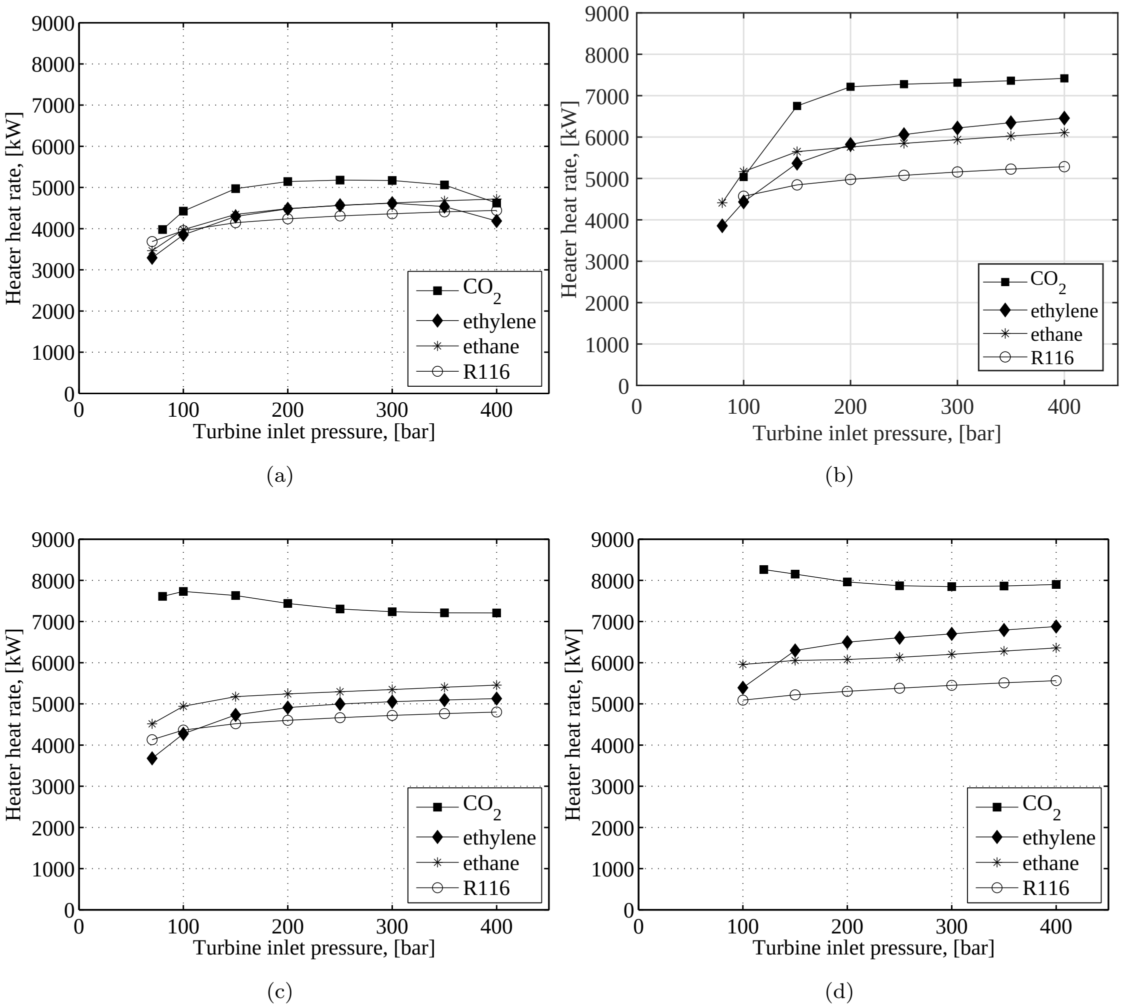

Figure 12: Effect of turbine inlet pressure on heater heat rate. Results presented in (a) are for simple cycle and (b) for intercooled cycle with higher CIT. Results presented in (c) are for simple cycle and (d) for intercooled cycle with lower CIT.

The results of cycle mass flow rates and fluid enthalpy change in the heater are presented in Figure 13. These results were obtained by using the simple cycle configuration and the lower compressor inlet temperature. From the studied fluids, R116 represents the highest mass flow rates of above 30 kg/s. The lowest working fluid mass flow rates less than 15 kg/s were simulated with ethane and ethylene. The observed deviations in the mass flow rates can be explained by the differences in the fluid enthalpy change in the heater as well as by the differences in the heater heat rates with different fluids. The fluids ethylene and ethane have the highest enthalpy change in the heater of the studied fluids. The working fluid mass flow rate is slightly lower and enthalpy change in the heater is higher with all the studied fluids when a high turbine inlet pressure is adopted in the cycle, in a comparison to the use of a lower turbine inlet pressure. It was observed that the cycle configuration and compressor inlet temperature do not have a significant effect on the working fluid mass flow rate or on the heater heat rate.

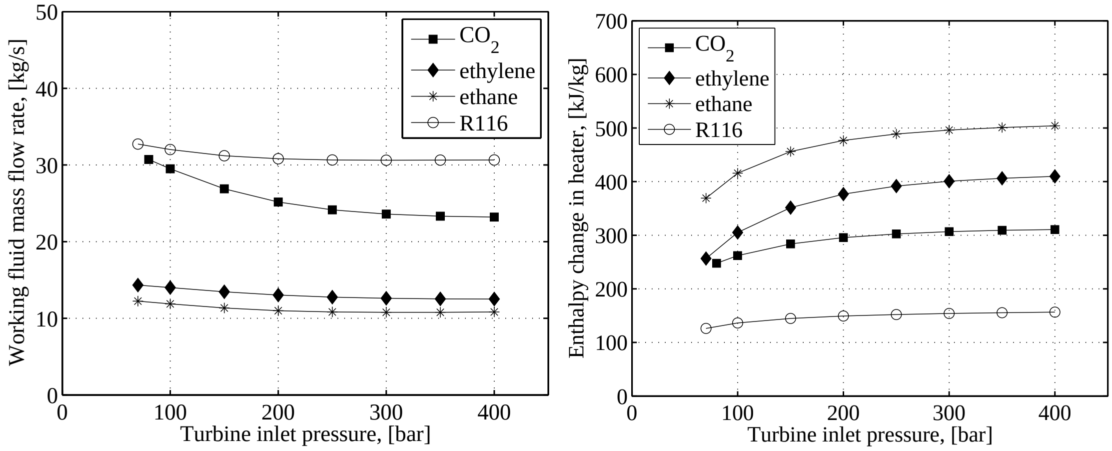

(a) (b)

Figure 13: Effect of turbine inlet pressure on working fluid mass flow rate (a) and fluid enthalpy change in heater (b). Results are presented for simple cycle with lower CIT.

The results of the cycle analysis are summarized in Table 7 showing the main process parameters resulted in the highest cycle performance for each of the studied case and each fluid.

4.3. Turbomachinery design analysis

As were observed in the sensitivity analysis, the cycle power output is highly sensitive on the efficiency of the cycle turbomachines. Thus, the turbomachinery design and turbine losses were studied in detail. The turbine efficiency prediction, turbine geometry and rotational speed were calculated for different operational conditions and fluids by combining the thermodynamic cycle model and the turbine design model. The turbine design was carried out by using the simple cycle configuration and CIT of 50 ^oC, but the selected cycle configuration and CIT have only minor effect on the turbine design. The simplified diagram representing the combined cycle and turbine calculation method is presented in Figure 14.

The results of the turbine rotational speed, rotor diameter, blade height at the turbine rotor inlet, and Mach number at the stator outlet are presented in Figures 15 a-d for different fluids and turbine inlet

Table 7: Summary of cycle analysis results representing the conditions with the highest simulated power output.

CO_2	Simple,CIT=50^{o}C	Simple, CIT=31^{o}C	Intercooled, CIT=50^{o}C	Intercooled, CIT=31^{o}C
P_e, [kW]	796.7	1671.6	1156.1	1758.6
η_e, [%]	15.5	23.2	15.8	22.3
$p_{t,in}$, [bar]	210.0	400.0	300.0	400.0
Π_t, [-]	2.8	5.4	4.0	5.4
$p_{t,out}$, [bar]	74.3	74.3	74.3	74.3
q_m, [kg/s]	27.3	23.2	23.3	22.8
P_c(total), [kW]	1536.6	1229.9	1397.2	1082.1
P_t, [kW]	2375.2	2989.4	2614.2	2933.2
ϕ_h, [kW]	5156.4	7209.4	7313.6	7900.3
$T_{eg,h,out}$, [^{o}C]	205.5	146.4	143.4	126.5

Ethylene	Simple,CIT=50^{o}C	Simple, CIT=30^{o}C	Intercooled, CIT=50^{o}C	Intercooled, CIT=30^{o}C
P_e, [kW]	612.0	857.9	980.3	1242.7
η_e, [%]	13.9	17.4	16.0	18.5
$p_{t,in}$, [bar]	175.0	210.0	270.0	305.0
Π_t, [-]	3.4	4.1	5.3	6.0
$p_{t,out}$, [bar]	50.9	50.9	50.9	50.9
q_m, [kg/s]	13.3	13.0	12.6	12.5
P_c(total), [kW]	1567.6	1537.0	1697.3	1570.1
P_t, [kW]	2211.8	2440.3	2729.2	2878.2
ϕ_h, [kW]	4406.8	4933.2	6128.7	6710.3
$T_{eg,h,out}$, [^{o}C]	227.1	212.0	177.5	160.8

Ethane	Simple,CIT=50^{o}C	Simple, CIT=33^{o}C	Intercooled, CIT=50^{o}C	Intercooled, CIT=33^{o}C
P_e, [kW]	721.2	1127.9	998.8	1316.4
η_e, [%]	16.0	21.0	16.8	20.7
$p_{t,in}$, [bar]	220.0	310.0	310.0	400.0
Π_t, [-]	4.5	6.3	6.3	8.1
$p_{t,out}$, [bar]	49.2	49.2	49.2	49.2
q_m, [kg/s]	11.0	10.8	10.8	10.9
P_c(total), [kW]	1263.0	1194.4	1330.0	1316.4
P_t, [kW]	2022.1	2381.7	2381.4	2702.
ϕ_h, [kW]	4520.5	5360.4	5954.6	6357.8
$T_{eg,h,out}$, [^{o}C]	223.8	199.7	182.5	170.9

R116	Simple,CIT=50^{o}C	Simple, CIT=30^{o}C	Intercooled, CIT=50^{o}C	Intercooled, CIT=30^{o}C
P_e, [kW]	635.9	839.0	799.8	988.9
η_e, [%]	14.7	17.7	15.4	17.8
$p_{t,in}$, [bar]	255.0	310.0	335.0	400.0
Π_t, [-]	8.2	10.0	10.8	12.9
$p_{t,out}$, [bar]	31.0	31.0	31.0	31.0
q_m, [kg/s]	30.7	30.6	30.6	30.6
P_c(total), [kW]	1231.7	1200.2	1317.5	1308.9
P_t, [kW]	1901.0	2083.3	2159.4	2349.8
ϕ_h, [kW]	4314.1	4729.6	5206.1	5565.7
$T_{eg,h,out}$, [^{o}C]	229.8	217.8	204.1	193.7

pressures. With all the studied fluids, the turbine optimal rotational speed is higher and the turbine wheel has smaller dimensions as the turbine design pressure at the inlet is increased. In general, the turbine rotational speeds are high, of tens of thousands of rpm, with all the studied fluids. The highest optimal rotational speeds were obtained with ethylene and ethane, while the use of R116 as the working fluid results in turbine design with the lowest rotational speeds. The use of ethylene and ethane results in turbine geometries having the smallest turbine diameters ranging from 0.07 m to 0.12 m, while the cycles using CO_2 or R116 represent slightly larger turbine wheels. These deviations in the optimal rotational speeds and geometry with different working fluids are due to the differences in the enthalpy drop over the turbine

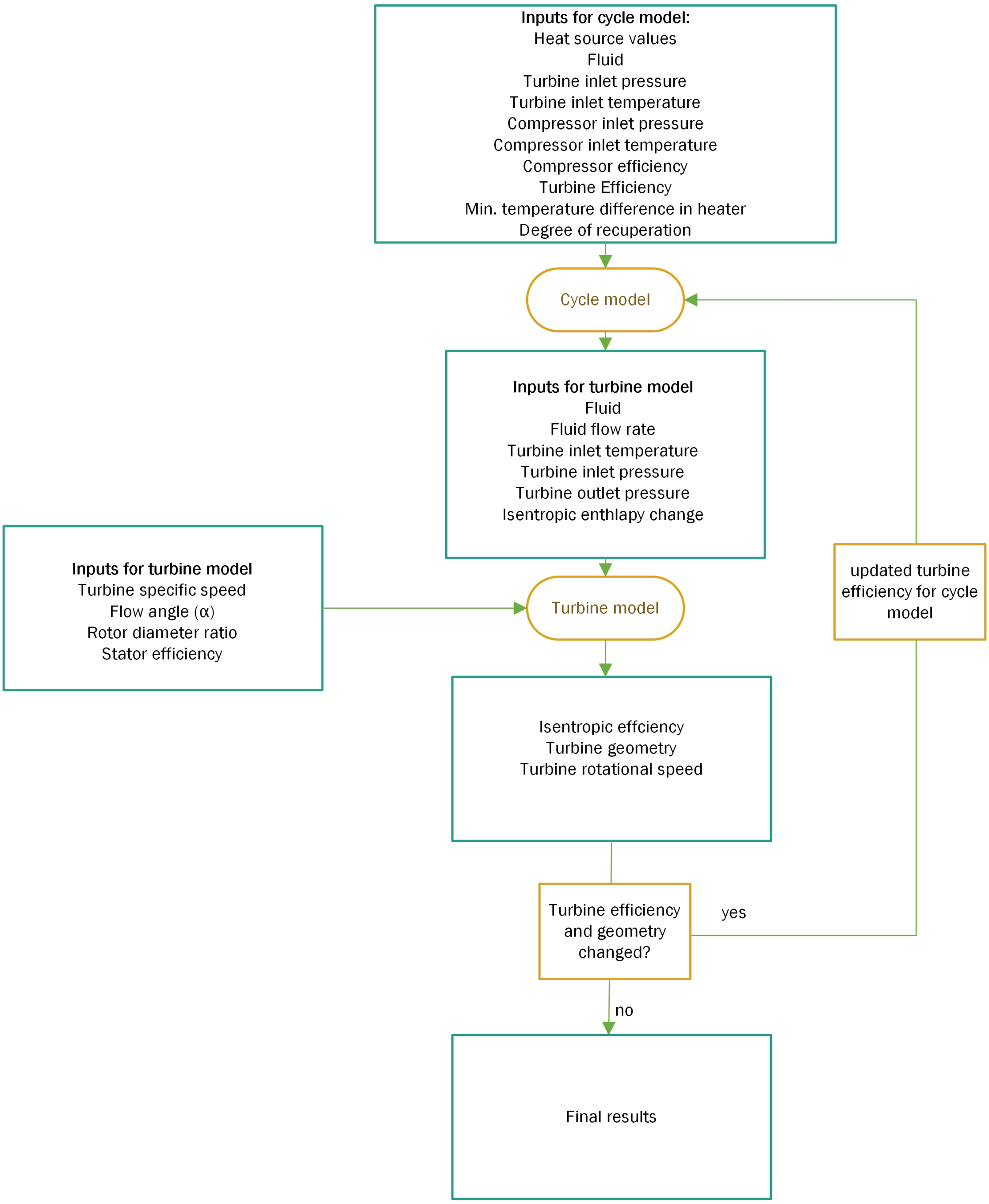

Figure 14: Simplified diagram of the combined cycle and turbine design model.

and different volumetric flow rates at the turbine outlet. According to the results, the designed turbines are significantly compact, when compared to for example ORC turbomachinery(e.g [38]). This can be considered as a beneficial feature especially in applications having restricted space for the WHR system. On the other hand, the high rotational speed, small dimensions and high pressures will set demands and challenges in the mechanical design of this type of turbogenerator, including requirements for the bearing and sealing solutions. The turbines designed by using CO_2 have the highest blade heights ranging from 5 to 15 mm depending on the turbine inlet pressure while the smallest blade heights were observed with ethane. The small blade height at the rotor inlet can lead to increased tip clearance losses. The use of CO_2 also resulted in lowest Mach numbers at the turbine stator outlet and the highest Mach numbers were observed with R116. The high Mach number increases the losses due to the presence of oblique shock waves inside the turbine. The flow velocity at the stator outlet was modelled to be supersonic with all the studied fluids, especially when a high turbine inlet pressure is adopted in the cycle.

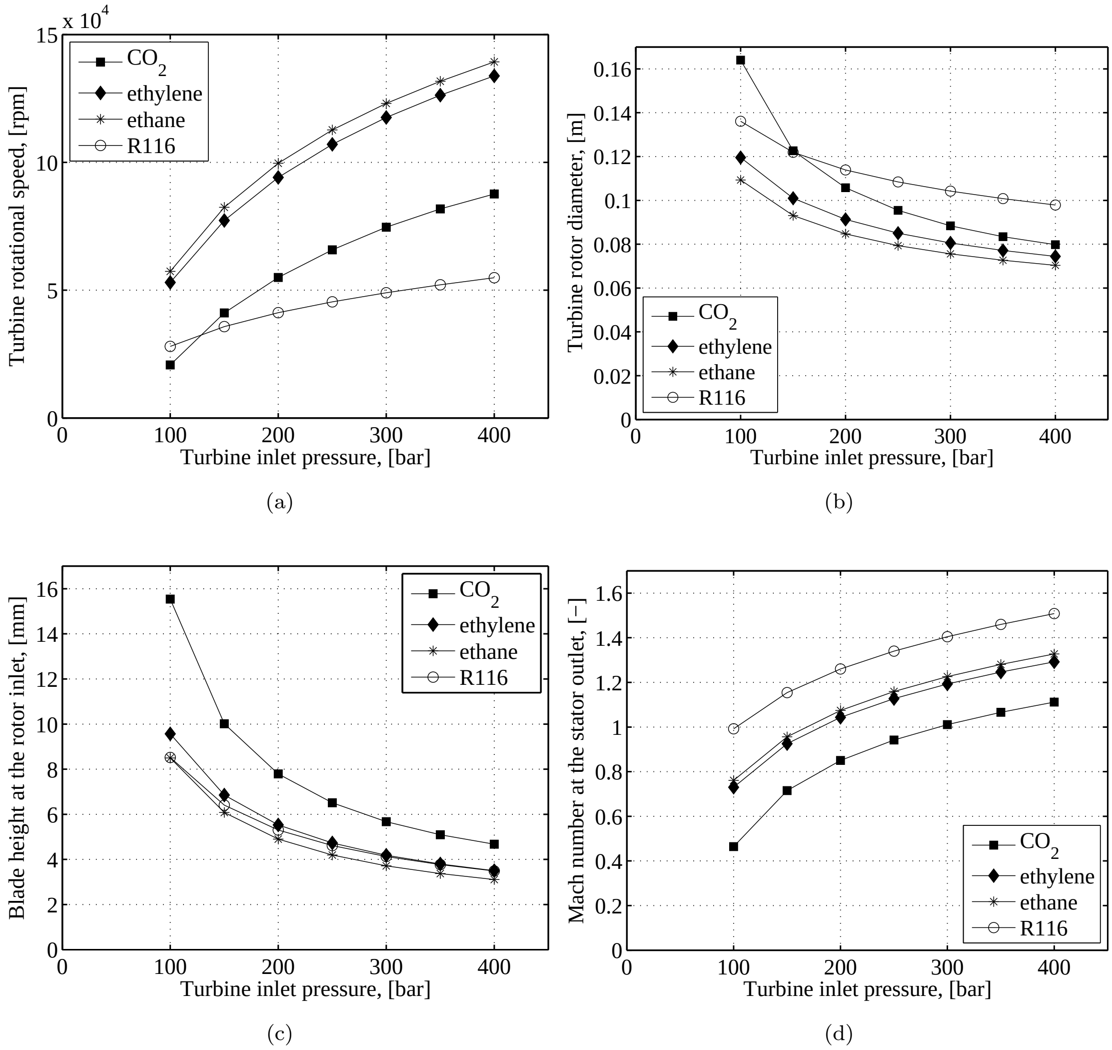

Figure 15: The turbine rotational speed (a), rotor diameter (b), blade height at the turbine rotor inlet (c), and Mach number at the stator outlet (d) with different turbine inlet design pressures.

The results for the predicted turbine isentropic efficiency, turbine passage loss, disk friction loss, and enthalpy drop over the turbine are presented in Figures 16 a-d. The simulated turbine efficiencies were significantly high, ranging from 90.5 to 91 % for all the studied fluids. The turbine efficiency is slightly lower when a high turbine inlet pressure is used compared to a turbine designed for lower turbine inlet pressure. In addition, both the passage loss and disk friction loss were estimated to increase as the turbine is designed for a high inlet pressure, but on the other hand, also the enthalpy drop over the turbine increases. The passage loss was estimated be more significant when compared to the disk friction loss with all the studied fluids and operational conditions. It should be noted, that in the efficiency prediction the stator efficiency was kept constant for all the fluids and operational parameters and only the passage loss and disk friction loss were included in the analysis. Thus, the turbine efficiencies presented here can be slightly over predicted. Especially with the turbine inlet pressures resulting in supersonic flow at the stator outlet, the turbine losses can be higher than presented here, due to the efficiency reductions related to the presence of shock waves. In addition, the tip clearance loss was not taken into account in the analysis, which can be a significant loss source in turbines, especially when the blade heights are significantly small at the rotor inlet.

The results of the compressor diameter are presented in Figures 17a and b. The blade height at the compressor wheel outlet are presented in Figures 17c and d. These results were obtained by using the simple configuration and both the higher and lower CIT. The designed compressor wheels have small diameters of less than 0.1 m in most of the studied cases and the designed compressor wheels are slightly smaller when compared to the respective turbine designs. The blade heights at the rotor outlet range from about 2 mm to 5 mm, except when using a low compressor outlet pressure. In general, the higher the compressor outlet pressure the smaller the blade height and compressor diameter. The small blade height can increase especially the tip clearance loss of the compressor, resulting in low compression efficiency, when a high compressor design outlet pressure is adopted. With R116 the largest compressor wheels were obtained but on the other hand the blade height is lower with this fluid when compared to the other studied fluids. With the highest compressor outlet pressures all the studied fluids have comparable blade heights at the rotor outlet and no significant deviations between the fluids were observed. It was also observed that the compressor inlet temperature has an effect on the optimal compressor wheel diameter caused mainly by the differences in temperature and enthalpy change over the compressor. On the other hand, differences in the simulated blade heights were almost negligible when comparing the designs carried out for cycles with different compressor inlet temperatures.

The compressor design for the intercooled cycle was also studied with CO_2 as the working fluid using the lower CIT and the results are compared against the results of the simple cycle compressor design. The results are presented in Figures 18a and b. In the intercooled cycle, as the compression is divided for two compressors the compressors wheels are smaller compared to the compressor design of the simple cycle. In addition, the specific speeds of the compressors are higher, in the range from 0.8 to 1.7, compared to the simple cycle, which can lead to reduced compression efficiency in the intercooled cycle. On the other hand,

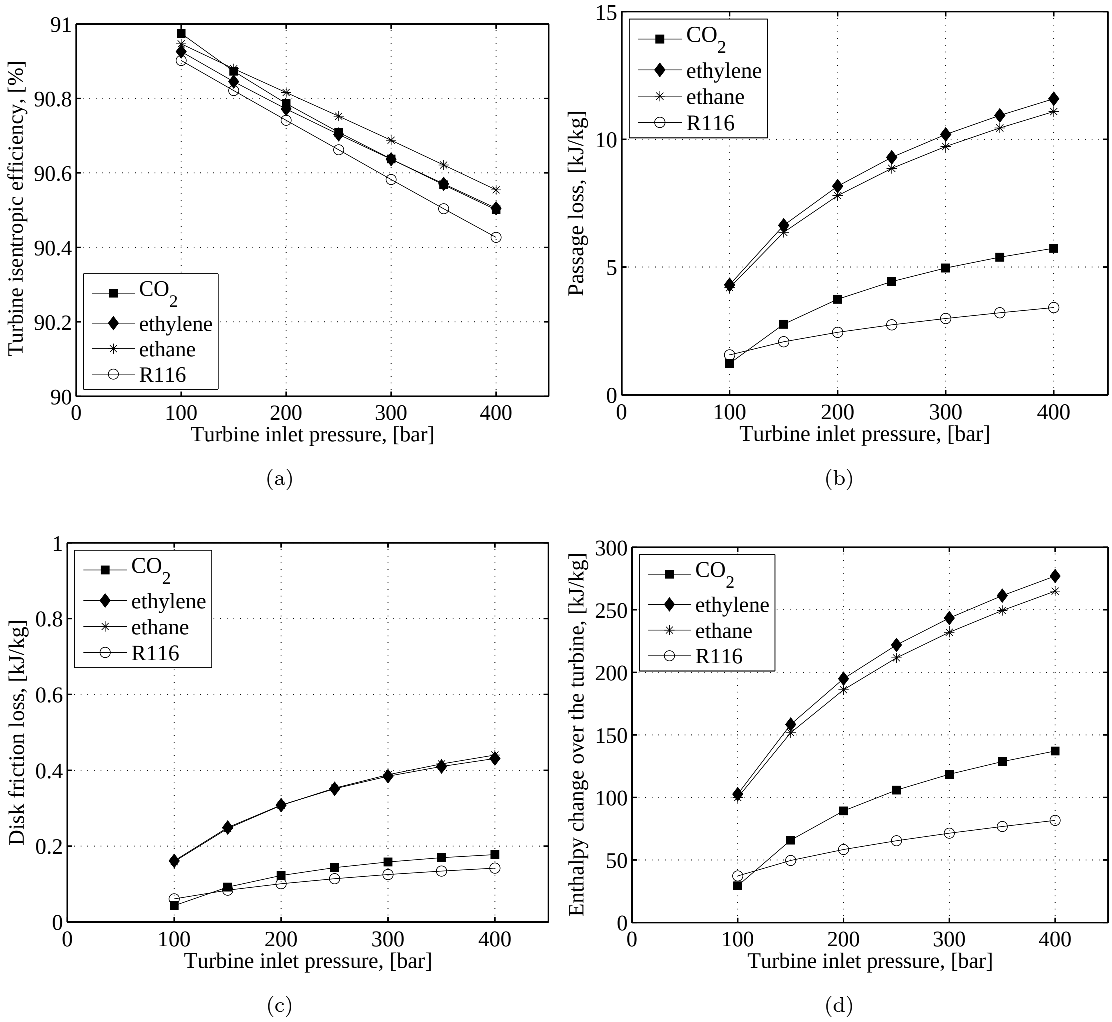

Figure 16: Predicted turbine efficiency (a), passage loss (b), disk friction loss (c), and enthalpy change over the turbine (d).

the blade height at compressor wheel outlet is higher when compared to the simple cycle, that can reduce the tip leakage losses. It should be noted as a general remark related to the compressor design, that if the compressor inlet state is close to the critical point a fluid condensation can occur in the compressor as the fluid is accelerated and this can cause erosion of the compressor wheel and reduce the compressor performance as a result of additional losses[49]. Thus, the lowest compressor inlet temperatures that were used in the study might cause problems related to flow condensation, and slightly higher compressor inlet temperatures could be considered due to this reason.

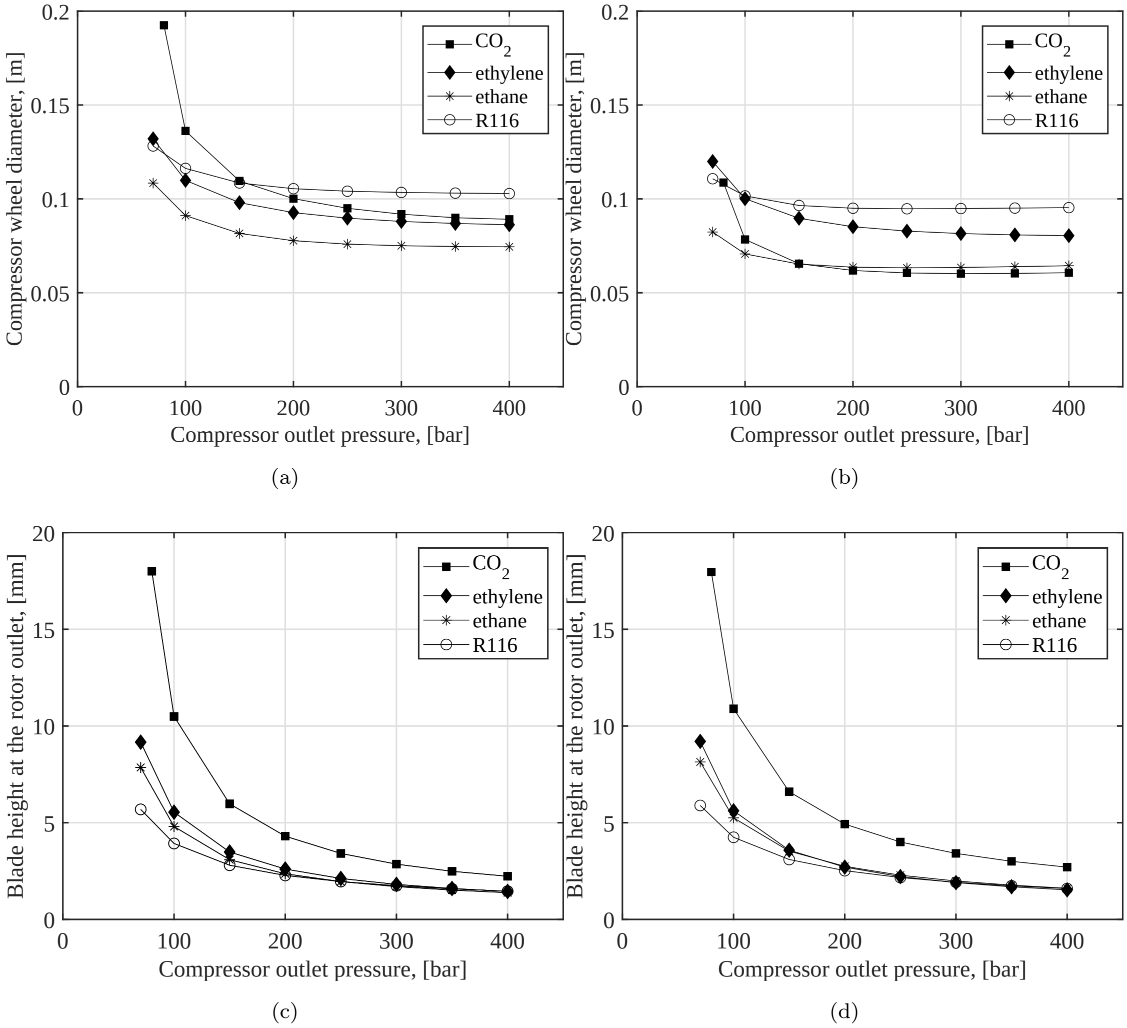

Figure 17: Compressor wheel diameter and blade height at the rotor outlet with different operation conditions and fluids. Results presented in (a) and (c) were obtained by using the higher CIT and (b) and (d) with the lower CIT.

5. Conclusions

The use of supercritical Brayton cycles for converting high temperature exhaust gas heat into electricity was investigated with different working fluids and two cycle layouts. Based on this study, the use of supercritical Brayton cycles can be considered as an attractive and efficient technological option for recovering high temperature exhaust gas heat and for increasing the energy efficiency and reduce emissions in engine power plants. The main conclusions drawn from the study are summarized as follows: • Supercritical Brayton cycles recovering high temperature waste heat are capable for increasing energy efficiency of large scale engines.

• CO_2 as the working fluid resulted in higher power outputs when compared to the other studied working

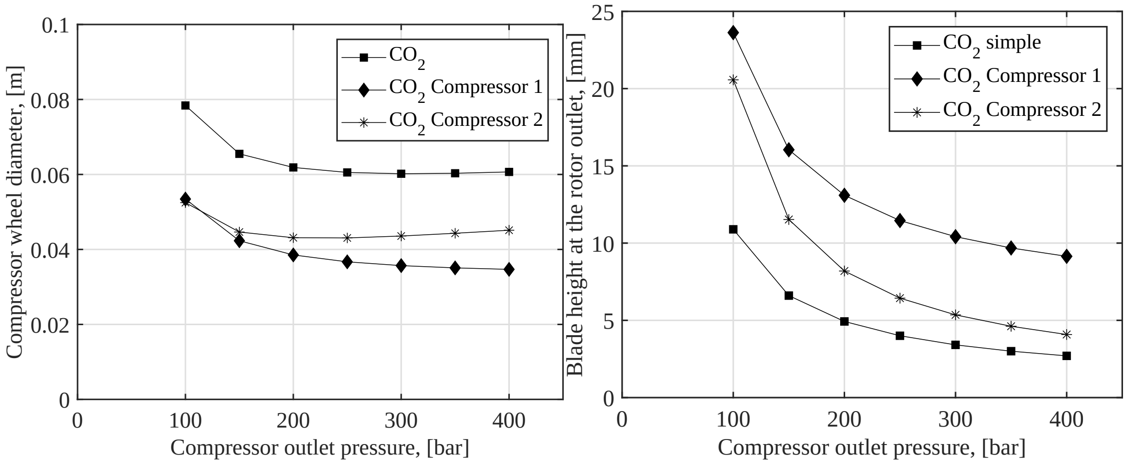

(a) (b)

Figure 18: Comparison of compressor wheel diameter and blade height at the rotor outlet with simple and intercooled SBC. Results were obtained by using the lower CIT and CO_2 as the working fluid.

fluids. The maximum power output of 1759 kW was simulated by using intercooled cycle layout and low compressor inlet temperatures. The simulated maximum power output corresponds to about 9,6 % of the engine power output.

• The use of ethane resulted in the second highest performances and R116 represented the lowest performance among the studied cases.

• The use of intercooled cycle resulted in higher power outputs when compared to the simple cycle. On the other hand, the cycle with intercooling is more complex when compared to the simple cycle.

• To reach high cycle performance, the system turbomachines have to be capable to operate with high efficiency and low compressor inlet temperature has to be used. Based on the detailed turbine design analysis, high turbine efficiencies of over 90 % can be reached.

• The system turbomachinery has very small dimensions and requirements for significantly high rotational speeds of tens of thousands rpm. As the turbine inlet pressure is increased, the optimal turbomachinery rotational speed increase and the wheel dimensions decrease. In most of the studied cycle conditions, the use of ethane resulted in smallest turbomachinery diameters and highest rotational speeds, while the use of R116 resulted in the largest turbomachines and the lowest rotational speeds.

• The use of significantly high turbine inlet pressure in a range of 200 bar to 400 bar is required to reach maximum thermodynamic performance. This sets special demands and challenges for the material strength and sealing solutions for such a system.

It was concluded that if the system turbomachines can be operated with high efficiency and low compressor inlet temperature can be used in the cycle, the power output is comparable to the high temperature ORC technology[4, 6]. In addition, this type of WHR system can be designed to be more compact when compared to ORC technology or conventional steam turbine cycles, especially when considering the size of the turbomachinery. This can be considered as a beneficial feature, especially in applications in where there is restricted space for the WHR system installation. The main drawbacks of the studied systems can be identified to be the significantly high pressure levels that sets special demands and challenges for the material strength and sealing solutions for such a system. In addition, the high rotational speeds and small dimensions of the turbomachinery disable the use of these WHR systems in rather low power output energy systems. In fact, despite that the analysis in this paper was carried out for relatively large engine having a power output of 18.3 MW, the design of reliable turbogenerators for this size systems can be challenging, especially due to the requirements for significantly high rotational speeds and extremely high power density. Thus, it was concluded that the studied WHR cycles have the greatest potential in large scale engine power plants in where the power output is in the range of tens of MW to hundreds of MW.

It should be noted that thermodynamics and fluid dynamics of non-conventional and supercritical fluids are not yet fully understood and investigated. It should be also noted that the loss correlations and turbomachinery design methods implemented in the analysis have been initially developed for turbomachines operating with ideal gases. Thus, the accuracy when considering the turbomachinery design and loss prediction with supercritical fluid conditions can contain high uncertainties, even though the real gas fluid properties were used in the analysis and the results were in a good agreement in the validation when compared to the different turbomachinery designs available in the literature. The authors highlight the importance of more experimental work to be carried out in the future for increasing the understanding of the main loss mechanisms, heat transfer and fluid dynamics effects of supercritical fluids and to develop more accurate performance prediction methods for the turbomachinery of this type of power systems. It is also recommended to study more complex cycle architectures for increasing the WHR system performance and to study the compressor losses and heat exchanger design with different fluids in detail in the future.

6. Acknowledgements

This study was conducted partly within the INTENS research project granted by Business Finland and partly by the funding of Lappeenranta University of Technology.

References

[1] Quoilin S, Van Den Broek M, Declaye S, Dewallef P, Lemort V. Techno-economic survey of Organic Rankine Cycle (ORC) systems. *Renewable and Sustainable Energy Reviews.* 2013;22:168-186.

[2] Sprouse III C, Depcik C. Review of organic Rankine cycles for internal combustion engine exhaust waste heat recovery. *Applied Thermal Engineering.* 2013;51(1-2):711-722.

[3] Colonna P, Casati E, Trapp C, Mathijssen T, Larjola J, Turunen-Saaresti T, Uusitalo A. Organic Rankine cycle power systems: from the concept to current technology, applications and an outlook to the future. *Journal of Engineering for Gas Turbines and Power*. 2015;137:10.1115/1.4029884.

[4] Bombarda P, Invernizzi CM, Pietra C. Heat recovery from Diesel engines: A thermodynamic comparison between Kalina and ORC cycles. *Applied Thermal Engineering*. 2010;30(2-3):212-219.

[5] Larsen U, Sigthorsson O, Haglind F. A comparison of advanced heat recovery power cycles in a combined cycle for large ships. *Energy*. 2014;74:260-268.

[6] Uusitalo A, Honkatukia J, Turunen-Saaresti T, Larjola J. A thermodynamic analysis of waste heat recovery from reciprocating engine power plants by means of organic Rankine cycles. *Applied Thermal Engineering*. 2014;70(1):33-41.

[7] Uusitalo A, Honkatukia J, Turunen-Saaresti T, Gronman A. Thermodynamic evaluation on the effect of working fluid type and fluids critical properties on design and performance of Organic Rankine Cycles. *Journal of Cleaner Production*. 2018;188:258-263.

[8] Lai NA, Wendland M, Fischer J. Working fluids for high-temperature organic Rankine cycles. *Energy*. 2011;36(1):199-211.

[9] Fernandez FJ, Prieto MM, Surez I. Thermodynamic analysis of high-temperature regenerative organic Rankine cycles using siloxanes as working fluids. *Energy*. 2011;36(8),5239-5249.

[10] Branchini L, De Pascale A, Peretto A. Systematic comparison of ORC configurations by means of comprehensive performance indexes. *Applied Thermal Engineering*. 2013;61(2):129-140.

[11] Maraver D, Royo J, Lemort V, Quoilin S. Systematic optimization of subcritical and transcritical organic Rankine cycles (ORCs) constrained by technical parameters in multiple applications. *Applied energy*. 2014;117:11-29.

[12] Schuster A, Karellas S, Aumann R. Efficiency optimization potential in supercritical Organic Rankine Cycles. *Energy*. 2010;35(2):1033-1039.

[13] Gao H, Liu C, He C, Xu X, Wu S, Li Y. Performance analysis and working fluid selection of a supercritical organic Rankine cycle for low grade waste heat recovery. *Energies*. 2012;5(9):3233-3247.

[14] Dostal V, Hejzlar P, Driscoll MJ. The supercritical carbon dioxide power cycle: comparison to other advanced power cycles. *Nuclear technology*. 2006;154(3):283-301.

[15] Iverson B, Conboy T, Pasch J, Kruizenga A. Supercritical CO2 Brayton Cycles for Solar-Thermal Energy. *Applied Energy*. 2013;111:957-970.

[16] Dostal V, Hejzlar P, Driscoll MJ. High-Performance Supercritical Carbon Dioxide Cycle for Next-Generation Nuclear Reactors. *Nuclear Technology*. 2006;154(3),265-282.

[17] Ahn Y, Bae SJ, Kim M, Cho SK, Baik S, Lee JI, Cha JE. Review of supercritical CO2 power cycle technology and current status of research and development. *Nuclear Engineering and Technology*. 2015;47(6):647-661.

[18] Li MJ, Zhu HH, Guo JQ, Wang K, Tao WQ. The development technology and applications of supercritical CO2 power cycle in nuclear energy, solar energy and other energy industries. *Applied Thermal Engineering*. 2017:126;255-275.

[19] Al-Sulaiman FA, Atif M. Performance comparison of different supercritical carbon dioxide Brayton cycles integrated with a solar power tower. *Energy*. 2015;82:61-71.

[20] Chen Y, Lundqvist P, Johansson A, Platell P. A comparative study of the carbon dioxide transcritical power cycle compared with an organic Rankine cycle with R123 as working fluid in waste heat recovery. *Applied Thermal Engineering*. 2006; 26(17):2142-2147.

[21] Hou S, Wu Y, Zhou Y, Yu L. Performance analysis of the combined supercritical CO2 recompression and regenerative cycle used in waste heat recovery of marine gas turbine. *Energy Conversion and Management*. 2017;151:73-85.

[22] Wang X, Dai Y. Exergoeconomic analysis of utilizing the transcritical CO2 cycle and the ORC for a recompression supercritical CO2 cycle waste heat recovery: A comparative study. *Applied Energy*. 2016;170:193-207.

[23] Dostal V, Driscoll MJ, Hejzlar PA. supercritical carbon dioxide cycle for next generation nuclear reactors. Doctoral

dissertation, Massachusetts Institute of Technology, Department of Nuclear Engineering. 2004.

[24] Wang Y. Guenette G. Hejzlar P. Driscoll MJ. Compressor Design for the Supercritical CO2 Brayton Cycle. 2004,AIAA Paper No. 2004-5722.

[25] Conboy T, Wright S, Pasch J, Fleming D, Rochau G, Fuller R. Performance characteristics of an operating supercritical CO2 Brayton cycle. *Journal of Engineering for Gas Turbines and Power*. 2012;134(11):111703.

[26] Seong GK, Jekyoung L, Yoonhan A, Jeong LL, Yacine A, Bockseong K. CFD Investigation of a Centrifugal Compressor Derived From Pump Technology for Supercritical Carbon Dioxide as a Working Fluid. *Journal of Supercritical Fluids*. 2014;86:160-171.

[27] Lee J, Baik S, Cho SK, Cha JE, Lee JI. Issues in Performance Measurement of CO2 Compressor Near the Critical Point. *Applied Thermal Engineering*. 2016;94: 111-121.

[28] Rovira A, Munoz-Anton J, Montes MJ, Martinez-Val JM. Optimization of Brayton cycles for low-to-moderate grade thermal energy sources. *Energy*. 2013;55:403-416.

[29] Invernizzi CM, van der Stelt T. Supercritical and real gas Brayton cycles operating with mixtures of carbon dioxide and hydrocarbons. Proceedings of the Institution of Mechanical Engineers, *Journal of Power and Energy*. 2012;226(5):682-693.

[30] Jeong WS, Lee JI, Jeong YH. Potential improvements of supercritical recompression CO2 Brayton cycle by mixing other gases for power conversion system of a SFR. Nuclear Engineering and Design. 2011;241(6):2128-2137.

[31] Utamura M, Hasuike H, Ogawa K, Yamamoto T, Fukushima T, Watanabe T, et al. Demonstration of supercritical CO2 closed regenerative brayton cycle in a bench scale experiment. GT2012-68697 ASME turbo expo, June 1115, 2012, Copenhagen, Denmark.

[32] Lemmon EW, Huber ML, McLinden MO. Reference fluid Thermodynamic and Transport Properties (REFPROP), Version 9.0, National Institute of Standards and Technology. 2010.

[33] Wärtsilä Engines 46DF Product guide

[34] Invernizzi C, Bonalumi D. Thermal stability of organic fluids for Organic Rankine Cycle systems: Chapter 5 in Organic Rankine Cycle (ORC) Power Systems: Technologies and Applications. Woodhead Publishing Series in Energy, 2016,Number 107. Editors: Macchi E., and Astolfi M.

[35] Angelino G, Invernizzi C. Real gas Brayton cycles for organic working fluids. Proceedings of the Institution of Mechanical Engineers, *Journal of Power and Energy*, 2001;215(1), pp:2738.

[36] Pasch J, Conboy T, Fleming D, Rochau G. Supercritical CO2 Recompression Brayton Cycle: Completed Assembly Description, Sandia National Laboratories, SANDIA REPORT 2012-9546. 2012.

[37] Vilim RB. Development and Validation of a Radial Inflow Turbine Model for Simulation of the SNL S-CO2 Split-Flow Loop, Argonne National Laboratory, ANL-ARC-195. 2011.

[38] van Buijtenen JP, Larjola J, Turunen-Saaresti T, Honkatukia J, Esa H, Backman J. Design and validation of a new high expansion ratio radial turbine for ORC application. 5th European conference on Turbomachinery. Prague, 2003,March 17-22.

[39] Kang SH. Design and experimental study of ORC (organic Rankine cycle) and radial turbine using R245fa working fluid. *Energy*. 2012;41(1):514-524.

[40] Wright SA, Radel RF, Vernon ME, Rochau GE, Pickard PS. Operation and analysis of a supercritical CO2 Brayton cycle. Sandia Report, No. SAND2010-0171. 2010.

[41] Balje OE. Turbomachines: A Guide to Design, Selection, and Theory. Wiley,New York. 1980.

[42] Rohlik H. Radial Inflow Turbines, Chapter 10 in Glassman AJ. Turbine Design and Application. 1972. Volume 1-3, NASA.

[43] Daily JW, Nece RE. Chamber dimension effects on induced flow and frictional resistance of enclosed rotating disks. Transactions of the ASME *Journal of Basic Engineering*. 1960;82: 217232.

[44] Balje OE. A contribution to the problem of designing radial turbomachines.Transactions of the ASME. 1952;74:451472.

[45] Lee J, Lee JI, Yoon HJ, Cha JE. Supercritical Carbon Dioxide turbomachinery design for water-cooled Small Modular Reactor application. *Nuclear Engineering and Design*. 2014;270:76-89.

[46] Dambach R, Hodson HP, Huntsman I. An Experimental Study of Tip Clearance Flow in a Radial Inflow Turbine. *Journal of turbomachinery*. 1999;121(4):644-650.

[47] Kim YM, Kim CG, Favrat D. Transcritical or supercritical CO_2 cycles using both low-and high-temperature heat sources. *Energy*. 2012;43(1):402-415.

[48] Uusitalo A. Working fluid selection and design of small-scale waste heat recovery systems based on organic Rankine cycles. Doctoral thesis, Lappeenranta University of Technology, Finland, 2014.

[49] Furusawa T, Miyazawa H, Yamamoto S. Numerical Method for Simulating Flows of Supercritical CO2 Compressor With Nonequilibrium Condensation. 2016. ASME Turbo Expo 2016. GT2016-56431, pp. V009T36A003.